

## THE KINEMATICS OF GLOBULAR CLUSTERS IN THE LARGE MAGELLANIC CLOUD

K. C. FREEMAN,<sup>1</sup> GARTH ILLINGWORTH,<sup>2,3</sup> AND AUGUSTUS OEMLER, JR.<sup>3,4,5</sup>

Received 1982 May 28; accepted 1983 March 8

### ABSTRACT

Velocities have been determined for 35 globular clusters in the LMC. These data have been combined with data from other sources to give velocities for 59 clusters ranging in age from  $\sim 10^8$  to  $\sim 10^{10}$  yr. The uncertainty in these mean velocities is typically  $10\text{--}20\text{ km s}^{-1}$ , small enough to allow a study of the kinematics-age relation for the LMC globular cluster system. Clusters younger than  $\sim 10^9$  yr are shown to have motions similar to the gas in their vicinity and to share the rotation solution previously found from H I velocity maps and H II region velocities. That is, these young clusters form a flattened system having a low line-of-sight velocity dispersion ( $\sim 15\text{ km s}^{-1}$ ), an amplitude for their rotation of  $37 \pm 5\text{ km s}^{-1}$ , a galactocentric systemic velocity of  $40 \pm 3\text{ km s}^{-1}$ , and a line of nodes in position angle  $1^\circ \pm 5^\circ$ , consistent with that found from previous kinematical and photometric studies. The older clusters (age  $\geq 1\text{--}2 \times 10^9$  yr) are also flattened to a disklike system with an intrinsic line-of-sight dispersion of only  $17\text{ km s}^{-1}$ , and a rotation amplitude of  $41 \pm 4\text{ km s}^{-1}$ . Surprisingly, however, both the systemic velocity at  $26 \pm 2\text{ km s}^{-1}$ , and the position angle of the line of nodes at  $41^\circ \pm 5^\circ$  are very significantly different for these older clusters. These differences remain when a transverse motion of the LMC of  $300\text{ km s}^{-1}$  toward the east, i.e., P.A.  $90^\circ$ , is included in the solutions. This enigmatic situation resisted all our valiant attempts at a solution.

While the number of clusters is small (only 9!), it was striking to note that even the oldest clusters in the LMC appeared to lie in a highly flattened disklike system with a  $z$  scale height  $z_0 \sim 0.5\text{ kpc}$  at  $r \approx 3^\circ \approx 3\text{ kpc}$ . Our data suggest that, quite unlike our own Galaxy, *there is no evidence for a kinematic halo population among the globular clusters in the LMC.*

*Subject headings:* clusters: globular — galaxies: Magellanic Clouds — galaxies: structure

### I. INTRODUCTION

The ages, kinematics, and chemical compositions of globular cluster systems in galaxies are of interest for their own sake and for what they can tell us about the formation history of a galaxy. In our Galaxy, the globular clusters are all about  $10^{10}$  yr old and were probably among the first objects to form. In the Magellanic Clouds, the globular cluster population is much more diverse. It includes clusters with a very wide range in age, from the “blue” globular clusters with ages of about  $10^7$  yr (these are structurally similar to the classical globular clusters: see Freeman 1980 for references) to the old halo-type clusters which are probably similar

in age to the clusters in our Galaxy (see Gascoigne 1980; Hodge 1981). This means that suitable conditions for globular cluster formation have prevailed in the Magellanic Clouds for a very long period, extending from the formation epoch of the Clouds themselves up to the present time. In our Galaxy, on the other hand, formation of globular clusters ceased long ago: no globular-like clusters are known with ages less than about  $10^{10}$  yr.

It would be very interesting to know why cluster formation occurred only very early in the Galaxy’s life, and not more recently. This would give some insight into the state of the forming galaxy at that time. However, the conditions in which globular clusters can form are not yet well understood. This is the particular importance of the Magellanic Cloud clusters. Globular clusters are still forming now in the Magellanic Clouds; they give us the opportunity to identify the conditions necessary for cluster formation, which exist now in the Magellanic Clouds but not now in the Galaxy.

In our Galaxy the cluster system is roughly spherical, with little net rotation: it is supported mainly by the random motions of the clusters, of about  $100\text{ km s}^{-1}$

<sup>1</sup>Mount Stromlo and Siding Spring Observatories, Research School of Physical Sciences, The Australian National University.

<sup>2</sup>Kitt Peak National Observatory, which is operated by the Association of Universities for Research in Astronomy, Inc., under contract with the National Science Foundation.

<sup>3</sup>Visiting Astronomer, Cerro Tololo Inter-American Observatory, which is supported by the National Science Foundation under contract AST 78-27879.

<sup>4</sup>Yale University.

<sup>5</sup>Alfred P. Sloan Foundation Fellow.

(Frenk and White 1980). In the inner parts of the system, there is a clear abundance gradient; in the outer parts, the abundance appears to be roughly uniform, in the mean, but has a spread of about 1 dex in Fe/H (Zinn 1980*a, b*). These facts suggest that the globular cluster system of the Galaxy formed early in the collapse of the proto-Galaxy, before dissipation had had a significant effect.

Much less is known about the Magellanic Cloud cluster systems. Although color-magnitude diagrams and abundances are available for several clusters, there is no overall picture yet of the chemical properties of the cluster systems, and the kinematical and structural properties of the cluster systems are not yet well established. For example, while it seems very likely that the young blue clusters in the LMC are kinematically associated with the extreme Population I, we need to know about the kinematics of the older red clusters: do they belong to a halo population, or are they part of the old disk? The purpose of this paper is to discuss this problem.

Until quite recently, the only extensive study of the kinematics of cloud clusters was by Ford (1970). Ford obtained velocities for 26 blue globulars and 10 red globulars in the Large Magellanic Cloud. He concluded that the blue clusters had the same kinematics as the young disk population, with a velocity dispersion of  $\sim 10 \text{ km s}^{-1}$ . However, this result was obtained only after applying a correction of  $37 \text{ km s}^{-1}$  to force the cluster velocities to agree, in the mean, with the disk velocities. This correction was necessary because of solar contamination of the spectra, most of which were taken near full moon. The spectra of the red globulars were taken under more favorable conditions and should have produced more reliable velocities. These suggest that the red clusters form a halo, with a velocity dispersion of about  $40 \text{ km s}^{-1}$ . Oddly, the center of mass velocity of the halo clusters seemed to be about  $25 \text{ km s}^{-1}$  less than that of the disk.

Andrews and Lloyd Evans (1972) have also published velocities for 15 young clusters, which, in general, have kinematics consistent with that of the Population I material.

Ford's results are suggestive, but more data are clearly needed in order to understand the kinematics of the cluster population in the LMC. For the past few years we have been engaged in such a study, and have obtained 117 usable spectrograms of 35 clusters. Simultaneously Cowley and Hartwick (1982) and Searle and Smith (1983) have been doing similar work. When our own data are combined with those of all other workers, we obtain velocities for 59 LMC clusters, covering a very wide range of ages. The distribution of these clusters over the LMC is shown in Figure 1.

In § II of this paper we describe the measurement and reduction of our velocities. In § III we discuss the published and unpublished work of others. Determina-

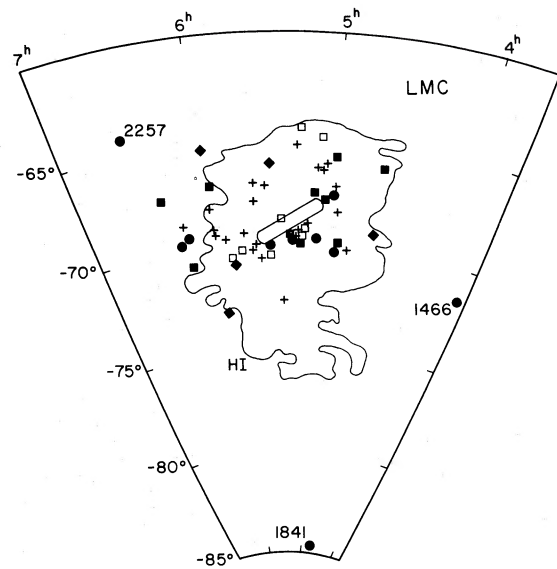


FIG. 1.—The distribution of globular clusters across the LMC. The outermost H I contour from McGee and Milton (1966) is shown, as is the position of the bar of the LMC. Young clusters (groups I–III from Table 5) are indicated by plus symbols, while the older clusters groups IV, V, VI, and VII, are shown by squares, filled squares, filled diamonds, and filled circles, respectively. The three old, outermost clusters, NGC 1466, NGC 1841, and NGC 2257 are indicated. Note how few clusters can be found in the S–SW sectors of the LMC.

tions of the ages of the clusters and of the local disk velocities at each cluster are described in § IV, and in § V we analyze the age and velocity data. In § VI we try to make some sense out of our peculiar findings.

## II. VELOCITY MEASUREMENTS

Internal velocities in the LMC are only a few tens of kilometers per second, and quite accurate velocity measurements are therefore needed. This is made difficult by the nature of the clusters. Although their integrated magnitudes are reasonably bright,  $10 < m_V < 14$ , many of the clusters, and in particular the red ones, are of quite low surface brightness. Indeed a few are of such low surface brightness that several hour exposures on a 4 m telescope of some 12th mag clusters produced spectrograms of very marginal quality. Besides the problem of low signal-to-noise ratio, the danger exists of velocity errors due to contamination by either solar light or the background disk light in the LMC. The former tends to lower the measured radial velocity, while the latter pulls the cluster velocity toward that of the disk. Ideally, a digital sky subtraction system should be used to minimize these problems. Unfortunately, during most of the course of this work, no such devices existed in the Southern Hemisphere, and all of our data reported in this paper were obtained photographically.

Spectrograms were obtained with the Cassegrain image tube spectrographs on the CTIO 1 m, 1.5 m, and 4 m telescopes, and the Mount Stromlo 1.8 m telescope. To minimize solar contamination, all cluster spectrograms were obtained during dark time with no moon. Dispersions used ranged from  $40 \text{ \AA mm}^{-1}$  to  $120 \text{ \AA mm}^{-1}$ . We attempted to obtain velocities of all the red clusters and of a reasonable sample of the more numerous blue clusters, but, because of their low surface brightness, we were unsuccessful with some of the red clusters. In the following sections, we discuss in detail the reduction of spectra from each of the telescopes.

#### a) CTIO 1.5 Meter Spectra

During an observing run on the CTIO 1.5 m telescope in 1974, spectrograms of 15 LMC clusters, four Galactic globular clusters, and 16 velocity standard stars were obtained at dispersions of  $39 \text{ \AA mm}^{-1}$  and  $78 \text{ \AA mm}^{-1}$ . The stars were chosen to cover a wide range (A5–G3) of spectral type from among those with accurate velocities listed in Abt and Biggs (1972). Because the stars were quite bright (typically  $m_V \sim 6$ ), neutral density filters were used to allow reasonable exposure times. The stars were trailed to produce spectra about 1 mm wide. The Galactic and LMC globulars were trailed somewhat and were also moved perpendicular to the slit during the exposure to minimize the contribution of single bright stars.

All spectra were scanned on the KPNO PDS and reduced to tables of intensity vs. log wavelength, using calibration spots obtained during the observing run. When a well exposed sky spectrum was present on a spectrogram of a LMC cluster, the sky spectrum was subtracted from that of the cluster. Often, however, the sky spectrum was underexposed, and adequate sky subtraction was not possible. Before analysis, the continuum of each spectrum was flattened by dividing it by a visually fitted curve.

The velocities of the stars were measured using the  $H\beta$ ,  $H\gamma$ ,  $H\delta$ , and  $H6$  lines of hydrogen, the Ca K line,  $\lambda 4226 \text{ \AA}$  of Ca I, and  $\lambda 4383 \text{ \AA}$  of Fe. The Ca H line and He were not used because they form a blend, whose effective wavelength is a function of spectral type. The wavelength of each line was measured by cross-correlating the spectrum in the neighborhood of each line with the same spectrum reversed. If the star had zero radial velocity, the cross-correlation would peak when the spectrum and the reverse spectrum were aligned at the rest wavelength of the line. The fractional shift in the position of the CCF peak from this point is twice the redshift.

After radial velocities were calculated from each line of each of the stars, it was apparent that there were systematic differences as large as  $36 \text{ km s}^{-1}$  in the velocities determined from different lines. The dif-

ference, averaged over all stars, between the velocity determined from a line and the mean velocity for all lines was applied as a correction to the velocity determinations from that line. This reduced the internal error and also corrected for velocity errors when a particular line was unmeasurable in a spectrum.

The rms internal error estimate of an individual velocity determination based on the scatter of corrected velocity measurements for the lines was  $9 \text{ km s}^{-1}$ . There was no significant difference in the errors for the three low-dispersion spectra and those for the 13 high-dispersion spectra. When the velocity determinations were compared with the published velocities of the stars, corrected for the Earth's motion, a strong pattern was evident. For stars with  $\alpha < 12^{\text{h}}$  which were observed at the end of the night, with the telescope in the west

$$\langle V - V_{\text{pub}} \rangle = +31 \pm 3 \text{ km s}^{-1}.$$

For stars with  $\alpha > 12^{\text{h}}$  observed at the beginning of the night, with the telescope in the east

$$\langle V - V_{\text{pub}} \rangle = +11 \pm 4 \text{ km s}^{-1}.$$

When the velocities in each group were corrected for this mean velocity shift, their scatter about the published velocities equaled that predicted from the internal errors.

The average difference of  $21 \text{ km s}^{-1}$  between the observed and true velocities is an entirely understandable instrumental shift. Indeed, since we shall measure cluster velocities relative to those of the stars it has no effect on our results. The shift of  $20 \text{ km s}^{-1}$  between the beginning and end of the night is more disturbing. Its most likely cause is magnetic effects within the image tube, which depend upon the relative positions of the telescope and observing platform. Since all stars were observed at extremes of time and hour angle, we cannot determine directly the velocity shift for small zenith distances where most of the clusters were measured. We shall assume that it is midway between those of the two groups of stars. Velocities for the Galactic globulars will provide a check on this assumption.

The velocities of all clusters were obtained by cross-correlating their spectra with the spectra of velocity standard stars. The spectra were divided up into 7 regions, covering wavelengths between  $3910 \text{ \AA}$  and  $4900 \text{ \AA}$ . Some regions are dominated by a few strong lines, while others contain many weak lines. The cross-correlations were performed in a fairly straightforward manner. The intensities were inverted (high values at the bottoms of lines, low values in the continuum) in order to give greatest weight to the cores of lines. Some subjective decisions had to be made about the centers of asymmetric cross-correlation functions, but they should have

TABLE 1  
VELOCITIES OF GALACTIC GLOBULAR CLUSTERS

NGC (1)	$V_{cl}^a$ (km s <sup>-1</sup> ) (2)	OBSERVED VELOCITY		
		1.5 m (km s <sup>-1</sup> ) (3)	1.0 m (km s <sup>-1</sup> ) (4)	4.0 m (km s <sup>-1</sup> ) (5)
104 ....	-14	-30 ± 8	...	-6 ± 10
362 ....	222	224 ± 13	225 ± 9	223 ± 7
1851 ....	316	...	298 ± 15	346 ± 13 <sup>b</sup>
1904 ....	185	197 ± 11	182 ± 14	191 ± 16
2808 ....	96	97 ± 6	...	96 ± 8
7089 ....	-6	...	...	22 ± 14 <sup>b</sup>
7099 ....	-172	...	...	-144 ± 10 <sup>b</sup>

<sup>a</sup>From Webbink (1981); see text.

<sup>b</sup>|Hour angle| ≥ 3<sup>h</sup>75 on 4 m.

little effect on the final velocities. The cluster spectra were cross-correlated with those of three stars: HR 5253 (spectral type F0), HR 4157 (type F5), and HR 176 (type G0). In neither these nor any other velocity measurements did we detect any systematic dependence of the derived velocity on the spectral type of the template star. To calculate cluster velocities, the true velocity of HR 176 was increased by 10 km s<sup>-1</sup>, and those of HR 4157 and HR 5253 were decreased by 10 km s<sup>-1</sup> to account for the velocity shift described above.

The results for Galactic globulars are presented in Table 1. Columns (1)–(3) list the cluster, its velocity as determined by previous workers, and the velocity determined from the 1.5 m spectra with 1  $\sigma$  error estimates based on the scatter of the velocities from the seven cross-correlations. In general, the velocity in column (2) is that given by Webbink (1981), but without the corrections to Kinman's (1959) velocities which Webbink applied. For the four clusters we find

$$\langle V_{1.5} - V_{pub} \rangle = 0 \pm 6 \text{ km s}^{-1}.$$

This excellent agreement gives us confidence that we have correctly handled the velocity shift problem. The standard deviation between observed and published velocities is 12 km s<sup>-1</sup>, very close to the value, 11 km s<sup>-1</sup>, predicted from the internal errors.

The velocities of the LMC clusters were measured in a manner identical to that used on the Galactic clusters. Of the 15 clusters, two were discarded because their spectra were too poor to measure. A spectrogram of one cluster, NGC 1835, although of good quality, gave a velocity which differed by 6  $\sigma$  from the well-determined mean of the other velocity measurements. We suspect that the wrong cluster was observed: the measurement has been discarded. The results for the other 12 clusters are presented in column (3) of Table 2. Typical internal errors are on the order of 20 km s<sup>-1</sup>.

#### b) CTIO 1.0 Meter Telescope Spectra

During an observing run in 1976, spectra were obtained of 10 stars, three Galactic globulars, and 10 LMC globulars with the Yale 1 m telescope at CTIO, at dispersions of 60 Å mm<sup>-1</sup> and 120 Å mm<sup>-1</sup>. Because of the excellent image tube on the 1 m telescope and the use of IIIa-J plates, these spectrograms were the highest quality obtained for this project.

The spectrograms were measured on the Yale PDS and reduced in a manner identical to that used for the 1.5 m spectra. Comparing velocities measured for the standard stars with their published velocities, we find

$$\langle V_{1.0} - V_{pub} \rangle = 0 \pm 8 \text{ km s}^{-1}.$$

There were no signs of systematic shifts within subsets of the stars. The random errors were slightly worse than those of the 1.5 m spectra: the internal error was 17 km s<sup>-1</sup>. The standard deviation between observed and published velocities was 25 km s<sup>-1</sup>.

The velocities of Galactic and LMC globulars were measured by cross-correlating with two stars: HR 176 (type G0) and HR 1502 (type F2). The results for the three Galactic globulars are presented in the fourth column of Table 1. We find

$$\langle V_{1.0} - V_{pub} \rangle = -5 \pm 6 \text{ km s}^{-1}.$$

As with the 1.5 m velocities, internal and external errors are comparable. The results for the LMC clusters are presented in column (2) of Table 2. Typical internal errors are ~15 km s<sup>-1</sup>, slightly better than for the 1.5 m velocities.

#### c) CTIO 4 Meter Telescope Spectra

During 1977 December spectra were obtained on the CTIO 4 m telescope of seven Galactic and eight LMC

globular clusters, at a dispersion of  $50 \text{ \AA mm}^{-1}$ . Despite the large telescope and the use of IIIa-J plates, these spectra are the poorest of all. In general, the clusters observed on the 4 m telescope were the most difficult objects (i.e., those with the lowest surface brightnesses) with which we had been unsuccessful on the smaller telescopes. Furthermore, because of the very diffuse light distributions of the clusters, the gain in observing them with larger telescopes is small. The spectra have other problems. The wavelength coverage only extends to  $4600 \text{ \AA}$ , losing two of our wavelength segments and, in particular, the strong  $H\beta$  line. Also, during the period of our run, the 4 m Cassegrain spectrograph suffered from serious wavelength shifts, which were dependent on both declination and hour angle (Cowley and Hartwick 1981*a*, 1982).

The spectra were measured and reduced in a manner similar to that described above, but with one complication. Because a very long slit was used, there is significant slit curvature on the spectrograms. This was calibrated using long-slit comparison line spectrograms obtained each night of the run. No velocity standard stars were observed; the two 1 m spectra of HR 176 and HR 1502 were used as the cross-correlation templates. This introduces the possibility of additional instrumental velocity shifts. We hoped to use the Galactic globulars to check for this.

Results for the Galactic globulars are presented in column (5) of Table 1. From these we find

$$\langle V_{4.0} - V_{\text{pub}} \rangle = +15 \pm 5 \text{ km s}^{-1}.$$

A shift of this size is quite reasonable to expect when using template stars from another telescope. Normally, this shift would be used to correct the velocities of the LMC clusters. We have not done so, for reasons which we shall discuss.

Results for the LMC clusters are listed in column (4) of Table 2. If one compares these velocities with the mean of all of our other measurements (except NGC 2193 for which only one other uncertain estimate is available) for each cluster one finds

$$\langle V_{4.0} - V_{\text{other}} \rangle = -33 \pm 15 \text{ km s}^{-1}.$$

Thus the Galactic and the LMC clusters suggest opposite velocity shifts for the 4 m spectra. The reasons are not clear. Cowley and Hartwick (1981*a*) have very kindly made available to us their calibration of velocity errors in the 4 m spectrograph. However, the corrections for the telescope positions at which our spectra were obtained are small. We suspect the spectrograph is to blame for our problems but have no consistent external measure of the true shifts. Therefore, the only unbiased procedure is to use the cluster velocities as observed, with no corrections.

#### d) Mount Stromlo 1.8 Meter Telescope Spectra

Spectra of LMC clusters were obtained at the Mount Stromlo 1.8 m telescope at a dispersion of  $100 \text{ \AA mm}^{-1}$  on a number of occasions between 1970 and 1979. The spectra fall into three groups, which were reduced in different ways. Nine spectra of red LMC globulars were obtained in two runs in 1979 during which four spectra of Galactic globular clusters were also obtained. The velocities of the Galactic globulars were measured by cross-correlating with the 1 m spectra of HR 176 and HR 1502. There were large systematic differences ( $6 \text{ km s}^{-1} < \Delta V < 72 \text{ km s}^{-1}$ ) between the true velocities and the velocities determined from individual wavelength regions, presumably due to instrumental effects. The LMC spectra were measured in the same way, and the shifts found from the Galactic globulars were used to correct the measured LMC velocities. Twenty-four spectra of red globulars were obtained on observing runs during which no velocity standards were observed. The entire set was measured in two ways. At Mount Stromlo they were measured on a single-axis spectral-line measuring engine, and velocities were derived by conventional techniques. At Yale they were measured on a PDS and cross-correlated with the two 1 m template spectra. A comparison of the two sets of velocities showed that

$$\langle V_{\text{Str}} - V_{\text{Yale}} \rangle = +5 \pm 9 \text{ km s}^{-1}.$$

The internal error estimates were also very similar, so the two sets of velocities were averaged. When compared with all of our other velocity measurements for each cluster, these velocities show a shift of

$$\langle V_{\text{Str}} - V_{\text{other}} \rangle = -12 \pm 9 \text{ km s}^{-1}.$$

The final reported velocities have, therefore, been corrected by  $+12 \text{ km s}^{-1}$ .

Forty-six spectra of blue LMC globulars were obtained over a number of years at  $100 \text{ \AA mm}^{-1}$ . These spectra were measured by conventional techniques at Mount Stromlo. No velocity standards were observed, and so the zero point of the velocity scale could not be checked directly for these clusters. However, a powerful independent check is available. In § V we compare the cluster velocities to the gas (H I) velocities at the position of the cluster. For the young clusters we will see that the velocity difference is small. For the youngest clusters in the Stromlo sample (groups I–III; see § IV) we find, in fact, that

$$\langle V_{\text{Str,B}} - V_{\text{H I}} \rangle = -6 \pm 7 \text{ km s}^{-1},$$

i.e., there appears to be no serious zero point error. This is supported by further consistency checks with the data of Andrews and Lloyd Evans (1972; see § III*c* below). All Mount Stromlo velocities are presented in column (5) of Table 2.

TABLE 2  
VELOCITIES OF LMC GLOBULAR CLUSTERS

NGC (1)	Observed Velocities				Other Velocities				
	1.0m km s <sup>-1</sup> (2)	1.5m km s <sup>-1</sup> (3)	4.0m km s <sup>-1</sup> (4)	Stromlo km s <sup>-1</sup> (5)	Ford km s <sup>-1</sup> (6)	Andrews Evans km s <sup>-1</sup> (7)	Cowley Hartwick km s <sup>-1</sup> (8)	Searle Smith km s <sup>-1</sup> (9)	<V> km s <sup>-1</sup> (10)
1466....	196±30 208±31	-	-	-	219±17	-	157±34	180±30	196±12
1644....	-	-	-	-	-	-	-	242±23	242±23
1652....	-	-	-	241±40	-	-	-	-	241±40
1711....	-	-	-	-	231±21	230±16	-	-	230±9
1749....	-	-	-	-	308±17	-	-	-	308±17
1751....	-	-	-	-	209±34	-	-	188±23	196±16
1754....	196±17	238±8	-	-	245±17	-	-	209±30	227±9
1755....	-	-	-	-	-	257±16	-	-	257±16
1774....	-	-	-	-	-	310±16	-	-	310±16
1783....	253±16	-	284±12	254±25 255±12 273±13	275±20	-	-	318±15	277±9
1786....	-	271±17	-	270±18 293±21	242±21	-	269±33	255±15	265±7
1805....	-	-	-	232±25 264±44 366±28 321±27 286±14 361±21	-	318±16	-	-	312±9
1806....	184±23 184±22	225±12	-	224±29 201±27 239±39	264±22	-	-	232±15	220±10
1810....	-	-	-	295±41 368±44 313±23	-	-	-	-	322±19
1818....	-	-	-	277±18 319±40 250±24 298±23 325±23 301±19	298±17	314±16	-	-	300±7
1831....	-	-	-	211±30 216±12 237±19 278±10	227±21	-	-	283±15	253±13
1835....	207±7	-	-	203±28 222±25 204±17 187±18	203±20	-	-	198±23	204±4
1841....	-	-	-	199±27	-	-	288±37	-	288±37
1846....	-	-	224±26	209±16 242±35	-	-	-	260±15	236±12
1850....	-	-	-	-	227±16	264±16	-	-	246±15
1854....	-	-	-	-	235±17	248±16	-	-	242±9
1856....	-	-	-	-	238±16	237±16	-	259±15	245±8
1866....	-	-	-	283±22 286±21 262±16	288±16	283±16	-	-	281±6
1868....	-	-	-	-	-	-	-	260±30	260±30
1872....	-	-	-	-	261±50	-	-	-	261±50
1885....	-	-	-	-	282±19	-	-	-	282±19
1898....	180±15	142±30	-	-	163±18	-	-	235±23	181±15
1903....	-	-	-	-	280±16	243±16	-	-	262±15
1917....	-	218±45	-	-	-	-	-	235±23	229±16
1944....	-	-	-	-	270±22	-	-	-	270±22
1953....	-	276±16	-	-	257±17	-	-	-	267±11
1978....	297±14	273±16	-	278±30 282±18	-	-	326±38	271±23	286±8
1987....	-	-	-	-	-	-	-	253±23	253±23
2004....	-	-	-	-	320±17	299±16	-	-	309±11
2019....	246±12 286±13	-	-	275±18	-	-	-	285±15	275±8

TABLE 2—Continued

NGC (1)	Observed Velocities				Other Velocities					$\langle V \rangle$ (10)
	1.0m km s <sup>-1</sup> (2)	1.5m km s <sup>-1</sup> (3)	4.0m km s <sup>-1</sup> (4)	Stromlo km <sup>-1</sup> (5)	Ford km s <sup>-1</sup> (6)	Andrews Evans km s <sup>-1</sup> (7)	Cowley Hartwick km s <sup>-1</sup> (8)	Searle Smith km s <sup>-1</sup> (9)		
2031....	-	-	-	-	242±26	-	-	-	242±26	
2041....	-	-	-	-	268±17	-	-	-	268±17	
2058....	-	-	-	-	263±21	-	-	-	263±21	
2065....	-	-	-	-	214±19	-	-	-	214±19	
2100....	-	-	-	-	253±17	280±16	-	-	267±13	
2107....	-	-	-	-	-	-	-	248±23	248±23	
2121....	-	-	184±20 206±23	240±27 264±23	-	-	-	210±30	219±15	
2134....	-	-	-	221±19 280±11 281±18 214±23	280±31	-	-	-	263±12	
2136....	-	-	-	273±46 223±19 223±36 221±15 212±35 211±22 247±35 226±32	274±23	-	-	-	238±16	
2154....	-	293±39	262±14	240±43	-	-	-	-	264±13	
2155....	347±17	-	250±35	258±22 284±29	-	-	251±39	264±23	284±15	
2156....	-	-	-	-	285±17	-	-	-	285±17	
2157....	-	-	-	317±17 264±33 230±18 324±38 267±24	284±19	266±16	-	-	276±8	
2164....	-	-	-	275±5 288±11	271±16	257±16	-	-	273±6	
2173....	287±23 313±25	203±25	198±12 162±10	254±39	-	-	-	-	232±22	
2193....	-	-	259±17 214±24 248±11	338±39	-	-	-	-	263±28	
2210....	-	323±20	-	298±26 334±18	315±17	-	251±36	325±15	313±10	
2213....	-	250±15	-	-	-	-	-	245±30	248±10	
2214....	-	-	-	272±6 281±41 298±23 358±14	279±20	-	-	-	289±10	
2231....	-	-	-	-	243±43	-	-	288±30	270±24	
2257....	-	-	320±53 239±13	310±41	-	-	304±36	-	284±19	
H-2 <sup>a</sup> ....	-	183±27	-	-	-	-	-	-	183±27	
H-11 <sup>a</sup> ....	-	-	-	351±35 211±21 317±36 264±88	-	-	228±48	236±25	249±16	
C1 132 <sup>b</sup> .	-	-	-	-	272±16	-	-	-	272±16	

NOTE.— $\langle V \rangle$  (col. [10]) is weighted mean of individual weighted means of observed data (cols. [2]–[5]) with other velocities (cols. [6]–[9]). All weights proportional to  $(\Delta V)^{-1}$ , i.e.,  $\langle V \rangle = [\sum(V_i/\sigma_i)]/[\sum(1/\sigma_i)]$ , while errors are derived from  $\Delta \langle V \rangle = (1/\sqrt{2})(n/[\sum(1/\sigma_i)]^2 + [\sum(V_i - \langle V \rangle)^2/\sigma_i^2]/[(n-1)\sum(1/\sigma_i)])^{0.5}$ .

<sup>a</sup>Anon 2 and Anon 11 are from Hodge (1960); also H2 is SL 363 and H11 is SL 868 (Shapley and Lindsay 1963).

<sup>b</sup>Designation from Ford 1970.

### III. OTHER VELOCITIES

#### a) Searle and Smith

Over the past few years, Searle and Smith (1983, hereafter SS) have been obtaining spectra of the older LMC clusters with the Intensified Reticon Scanner on

the DuPont 100 inch (2.54 m) telescope at Las Campanas. These observations have the very great advantage over our spectra in having been obtained with a digital sky-subtracting detector. They should, therefore, be free of problems of velocity errors due to sky contamination. Drs. Searle and Smith have been extremely

generous in allowing us to use their velocities in advance of publication.

Searle and Smith have usually obtained several spectra of each cluster. The means of their velocity determinations are presented in column (9) of Table 2. Searle (1981) noted that the zero point uncertainty for the SS velocity system is  $\sim 15 \text{ km s}^{-1}$ . When we compare the SS velocities with our own we find

$$\langle V_{\text{SS}} - V_{\text{FIO}} \rangle = +6 \pm 7 \text{ km s}^{-1}.$$

The absence of a significant zero point shift between our velocities and Searle and Smith's is very gratifying, since it indicates that our velocities are also free from contamination problems. In addition since these data were taken with several telescopes, and independently reduced this result indicates that the zero point uncertainty for the older clusters is probably  $< 15 \text{ km s}^{-1}$ .

#### b) Ford Velocities

Ford (1970) obtained spectra at a dispersion of  $46 \text{ \AA mm}^{-1}$  on the CTIO 1.5 m telescope of 10 red and 26 blue clusters in the LMC. For the red clusters he obtained an average of two spectra per cluster. These were obtained under generally reasonable observing conditions, with little or no moonlight. Ford's individual cluster velocities,  $V_i$ , were averaged, weighed by  $(1/\text{P.E.})$ , where P.E. is the uncertainty associated with each velocity measure. This procedure resulted in less subjective weights and less sensitivity to poorly determined error estimates than Ford's approach (see also the discussion in § IIIe). Our weighted average velocities for Ford's clusters are presented in column (6) of Table 2. The error estimates are not those given by Ford. Their derivation is discussed in § IIIe. Comparing Ford's velocities with the mean of our velocities and the SS velocities, we find

$$\langle V_{\text{F}} - V_{\text{other}} \rangle = +6 \pm 8 \text{ km s}^{-1}.$$

Therefore, the velocity systems of Ford, Searle and Smith, and ourselves, seem to be in agreement.

As mentioned earlier, Ford's spectra of blue globulars were taken near full moon, and many are badly contaminated by the solar spectrum. Ford found that the rotation curve for the LMC determined from the blue clusters was shifted by  $-35 \text{ km s}^{-1}$  relative to that of the gas, a plausible result of the solar contamination. If we compare Ford's blue cluster velocities with velocities for the same clusters by SS and ourselves, we find

$$\langle V_{\text{F,B}} - V_{\text{other}} \rangle = -29 \pm 7 \text{ km s}^{-1},$$

a shift similar to that found by Ford. One would think that Ford's better spectra—those of individual supergiants in two clusters and the less contaminated cluster

spectra—would show a smaller velocity shift. Curiously, this is not so; the better spectra, if anything, show a larger shift. We have therefore, applied a shift of  $+29 \text{ km s}^{-1}$  to all of Ford's blue cluster velocities. These corrected values are also presented in column (6) of Table 2.

#### c) Andrews and Lloyd Evans

Andrews and Lloyd Evans (1972, hereafter AE) obtained spectra of 14 blue LMC clusters at  $86 \text{ \AA mm}^{-1}$  and  $170 \text{ \AA mm}^{-1}$  on the 1.9 m Radcliffe telescope. When their velocities are compared with the mean of ours, Searle and Smith's, and Ford's (corrected) we find

$$\langle V_{\text{AE}} - V_{\text{other}} \rangle = +2 \pm 6 \text{ km s}^{-1}.$$

These velocities, uncorrected for any shifts are presented in column (7) of Table 2.

#### d) Cowley and Hartwick

Cowley and Hartwick (1982, hereafter CH) have obtained spectra of 25 individual giant stars in eight LMC clusters, at a dispersion of  $90 \text{ \AA mm}^{-1}$  on the CTIO 4 m telescope. Their mean velocities are presented in column (8) of Table 2. Comparing the CH velocities with the mean of all other velocity determinations for the same clusters we find

$$\langle V_{\text{CH}} - V_{\text{other}} \rangle = -15 \pm 16 \text{ km s}^{-1}.$$

The uncertainty is large, but there is no significant difference in the velocity systems.

#### e) Errors

It is very gratifying that, with the exception of Ford's badly contaminated blue cluster velocities, all of the velocity systems of all workers are in good agreement. The excellent agreement between the digitally obtained SS velocities and the others is particularly reassuring. Considering this, and considering the good agreement of published velocities and our velocities for Galactic globulars, we think it unlikely that the combined data will have systematic errors greater than  $\sim 5 \text{ km s}^{-1}$ .

The random errors require more consideration. It is a well-known fact that errors quoted for radial velocities are often substantially (typically a factor of 2) smaller than the true errors. We shall test for such an effect among our data by comparing various sets of velocity determinations. We first compare the mean velocity (calculated in a manner to be discussed later) of each cluster from our measurements with the corresponding SS velocity. The standard deviation of the velocity difference for 17 clusters is

$$\sigma(\text{SS}/\text{FIO}) = 31 \text{ km s}^{-1}.$$

Our quoted error for an individual velocity measurement is the standard deviation of the mean of the velocities determined from the cross-correlation of each of the seven spectrum segments. The error of the mean of all of our velocities for a cluster is calculated in a manner described below. For the SS velocities, we use the error estimate provided to us by Drs. Searle and Smith and listed in column (9) of Table 2. From these error estimates we predict

$$\sigma_p(\text{SS/FIO}) = 28 \pm 5 \text{ km s}^{-1}.$$

Our error estimates, and those of SS, appear to be in good agreement.

We now combine our data and the SS data and compare it to the Ford velocities for red clusters. We find

$$\sigma(\text{FIO} + \text{SS}/\text{Ford}) = 25 \text{ km s}^{-1}.$$

Using Ford's error estimates, we predict

$$\sigma_p(\text{FIO} + \text{SS}/\text{Ford}) = 18 \pm 4 \text{ km s}^{-1}.$$

Thus, Ford's quoted errors appear to be too low. This is not surprising as some are implausibly small, as Ford himself noted (e.g.,  $\pm 1 \text{ km s}^{-1}$  for NGC 1754).

We, therefore, calculate new error estimates for Ford's red cluster velocities:

$$\sigma^2(\text{Ford}) = \sigma_q^2 + (17 \text{ km s}^{-1})^2,$$

where  $\sigma_q$  is Ford's quoted error. These new errors are listed in column (6) of Table 2.

Similarly, comparing our and SS's velocities to Ford's blue cluster velocities, after correcting for the zero point, we find

$$\sigma(\text{FIO} + \text{SS}/\text{Ford}) = 23 \text{ km s}^{-1}$$

$$\sigma_p(\text{FIO} + \text{SS}/\text{Ford}) = 17 \pm 3.5 \text{ km s}^{-1}.$$

We, therefore, correct the quoted errors by adding  $16 \text{ km s}^{-1}$  in quadrature to the blue cluster errors, listing the new errors also in column (6).

Now, combining Ford's corrected velocities with our own and Searle and Smith's, we compare them with those of Andrews and Lloyd Evans and get

$$\sigma(\text{other}/\text{AE}) = 22 \text{ km s}^{-1}$$

we predict

$$\sigma_p(\text{other}/\text{AE}) = 15 \pm 3 \text{ km s}^{-1}.$$

Therefore we add  $16 \text{ km s}^{-1}$  in quadrature to the

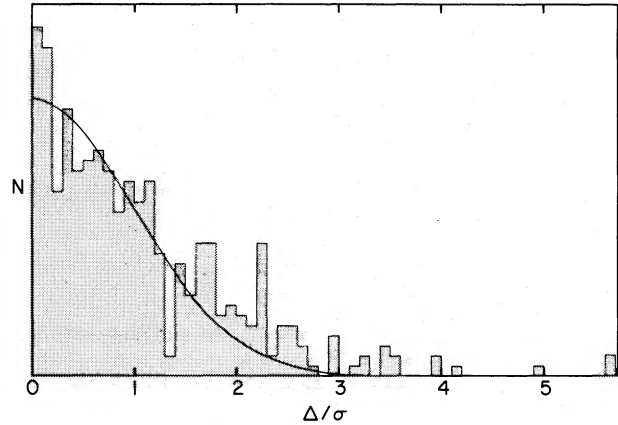


FIG. 2.—Comparison of external,  $\Delta$ , to internal,  $\sigma$ , error estimates, where  $\Delta$  is determined from a pairwise comparison of the velocity measurements for each cluster in Table 2. The expected, normal distribution of  $\Delta/\sigma$  with unit variance is shown. While the actual and expected distributions are similar for  $\Delta/\sigma \leq 2$ , an excess of large deviations  $\Delta/\sigma \geq 2.5$  is apparent.

quoted Andrews and Evans errors. These corrected errors are listed in column (7) of Table 2.

Finally, we combine all of the data discussed so far and compare it to the Cowley-Hartwick velocities. Leaving out NGC 2210 and H11, because of their very large discrepancy and large error respectively, we find

$$\sigma(\text{other}/\text{CH}) = 39 \text{ km s}^{-1}.$$

Using the CH published errors we predict

$$\sigma_p(\text{other}/\text{CH}) = 22 \pm 7 \text{ km s}^{-1}.$$

To correct the CH errors, we add  $32 \text{ km s}^{-1}$  in quadrature. These new errors are listed in column (8) of Table 2.

In the mean, the errors quoted in Table 2 should be a fair estimate of the true errors. To test this, we compare the velocity differences,  $|\Delta|$ , between each pair of velocity measurements for a cluster with

$$\sigma_p = (\sigma_i^2 + \sigma_j^2)^{1/2}.$$

The ratio of these two quantities,  $|\Delta|/\sigma_p$ , should be normally distributed with unit variance. The actual and expected distributions are presented in Figure 2. The two distributions are similar for small deviations,  $|\Delta|/\sigma_p < 2.0$ , but there are many more large ( $|\Delta|/\sigma_p > 2.5$ ) deviations than predicted.

Because the errors  $\Delta V$  are not perfectly represented by a normal distribution, we have chosen to form a mean by weighing the velocity measures by  $1/(\Delta V)$  rather than  $1/(\Delta V)^2$ . These means, with the ap-

propriately calculated errors, are presented in the last column of Table 2.

#### IV. OTHER CLUSTER DATA

In order to use the clusters' kinematics to learn about the formation history of the LMC, we need two additional pieces of information about each cluster. We obviously need its age; we also need, in order to compare the kinematics of the cluster with the youngest material, the velocity of the disk gas and the youngest stars at each cluster's projected location. In this section we gather that data.

##### a) Cluster Ages

The ages of clusters in the Magellanic Clouds present a difficult problem. Because of the Clouds' distance, photometry down to the main sequence turnoff of the old clusters is very difficult and has, so far, only been obtained in one cluster, NGC 2257 (Stryker 1981). A few other red clusters have photometry sufficiently far down the giant branch to ensure that they are older than  $\sim 5 \times 10^9$  yr, and complete color-magnitude diagrams exist for a number of the younger clusters. However, for most, the age can only be estimated indirectly.

Searle, Wilkinson, and Bagnuolo (1980) have used Gunn system photometry of 61 cloud clusters to construct two reddening-free color indices. They find that in this two-color plane the clusters form a one-dimensional sequence which they interpret as a sequence of age (and also metallicity). They divide the sequence into seven segments, denoted I through VII. Segments I–V represent a sequence of cluster ages running from very young to those a few billion years old. Region VII is occupied only by old ( $\sim 10^{10}$  yr) relatively metal-poor clusters, while the clusters in region VI are either old, less metal-poor objects, or somewhat younger objects. Searle, Wilkinson, and Bagnuolo (1980, hereafter SWB) classifications for our clusters are presented in column (2) of Table 3.

Although SWB types are only available for 40 of our clusters, we can do almost as well using  $UBV$  colors. In Figure 3 we plot the location and types of the SWB clusters in the  $U - B/B - V$  plane. This distribution is very similar to that in Figure 3 of SWB.  $U - B$  and  $B - V$  colors of the clusters taken from van den Bergh (1981) are presented in columns (3) and (4) of Table 3. Using these and the dividing lines between types shown in Figure 3 we derive types for all clusters. These are presented in column (5).

Aaronson and Mould (1982) present infrared photometry of asymptotic giant branch stars in a number of cloud clusters. Using their theory for the relation between the brightest extent of the asymptotic giant branch and the cluster age, they derive ages for a number of clusters. These are listed in column (6) of Table 3. The

presence of RR Lyrae stars is thought to indicate that a cluster is at least  $5 \times 10^9$  yr old. Clusters in which RR Lyrae stars have been found (Graham 1973; Thackeray 1974) are noted in column (7).

Finally, also in column (7), we summarize available age determinations from color-magnitude diagrams, the sources for which are listed in the footnotes to Table 3. Age estimates for clusters without colors are given in column (7), usually from comparisons of spectral types with other age-dated clusters as noted.

Using all of the available information we have divided the clusters into age groups, corresponding roughly to SWB groups I–VII. These are listed in the last column of Table 3. The details of this age grouping are not critical for the discussion that follows.

##### b) Disk Kinematics

There are three components of extreme Population I for which observations exist in the LMC: H II regions, supergiants, and H I. The H I velocity field has been extensively mapped by McGee and Milton (1966) at 21 cm. The resolution of their survey is  $\sim 15'$  and their coverage,  $4^{\text{h}}30 < \alpha < 6^{\text{h}}20$ ,  $-64^\circ < \delta > -78^\circ$ , spans the entire area over which H I is detectable, down to a brightness temperature of 4.4 K.

The H I kinematics are, unfortunately, rather complex. Over the greater part of the face of the galaxy the gas does follow a smooth rotation curve. However, in some regions there are multiple velocity peaks, and in some places there are strong velocity shears which make the true disk velocity ambiguous. Particularly bad is the region around  $5^{\text{h}}45$ ,  $-71^\circ$ , where the H I velocity suddenly rises by  $40 \text{ km s}^{-1}$ , producing a high-velocity region which is not consistent with smooth, circular rotational velocities.

In some cases, observations of H II regions and supergiants are helpful in resolving uncertainties about the true disk velocity. Both, in general, show a very small dispersion, about  $5 \text{ km s}^{-1}$  about the gas velocity. Prevot (1973) has measured velocities for about 150 supergiants in the LMC. Feast (1968), Cheriguene and Monnet (1972), and Smith and Weedman (1971) have measured velocities for a comparable number of H II regions. However, because the distribution of these objects over the face of the LMC is not as extensive as that of the H I, some areas of ambiguity remain.

Velocities for the gas or supergiants at the projected position of each cluster are presented in column (3) of Table 4. Velocities were estimated to the nearest  $5 \text{ km s}^{-1}$ . Where problems exist, they have been noted. Some of the older clusters are beyond the observed H I disk. For some of these, disk velocities have been estimated by extrapolating velocity trends seen in the H I. Unless there are drastic discontinuities in the velocities, this should be safe.

TABLE 3  
COLORS AND AGES FOR LMC GLOBULAR CLUSTERS

NGC (1)	T <sub>SWB</sub> (2)	U-B (3)	B-V (4)	T <sub>UBV</sub> (5)	t <sub>g</sub> (AM) (6)	t <sub>g</sub> (7)	T (8)
1466....	VII	0.13	0.66	VII	...	12 <sup>a</sup>	VII
1644....	V	0.21	0.62	V	...	...	V
1652....		0.32	0.85	VI	old?	...	VI
1711....	II	-0.37	0.12	II	...	...	II
1749....	...	...	...	...	...	II: <sup>b</sup>	II(?)
1751....	V	0.40	0.82	V	1.0	...	V
1754....	...	0.18	0.74	VII	...	...	VI
1755....	II-III	-0.21	0.15	II	...	...	II
1774....	II	-0.27	0.20	II	...	...	II
1783....	V	0.23	0.62	V	<3	...	V
1786....	...	0.10	0.74	VII	...	...	VII
1805....	...	-0.55	0.11	I	...	...	I
1806....	V	0.26	0.73	V	1.6	...	V
1810....	...	-0.51	0.22	I	...	...	I
1818....	I	-0.47	0.18	I	...	0.017	I
1831....	V	0.13	0.34	IV	<2.5	0.2	IV-V
1835....	VII	0.16	0.73	VII	...	a	VII
1841....	VII	0.50	0.90	V	old?	12	VII
1846....	V	0.31	0.75	V	2	...	V
1850....	...	-0.35	0.12	II	...	0.05	II
1854....	II	-0.22	0.21	II	...	0.03	II
1856....	IV	0.07	0.34	IV	...	0.08	IV
1866....	III	-0.04	0.25	III	...	0.08	III
1868....	...	0.15	0.45	IV	...	0.4-0.7	IV
1872....	III-IV	0.06	0.35	IV	...	...	IV
1885....	...	-0.05	0.38	III-IV	...	...	III-IV
1898....	...	0.03	0.74	VII	...	...	VII
1903....	II	-0.25	0.14	II	young	...	II
1917....	...	0.31	0.66	V	...	...	V
1944....	...	...	...	...	...	III: <sup>c</sup>	III(?)
1953....	...	0.07	0.25	IV	...	...	IV
1978....	VI	0.23	0.78	VI	2	...	VI
1987....	IV	0.20	0.52	IV	1.6	...	IV
2004....	I	-0.68	0.17	I	...	0.007	I
2019....	VII	0.18	0.75	VII	>6	...	VII
2031....	...	-0.05	0.27	III	...	...	III
2041....	III	-0.17	0.22	III	...	...	III
2058....	III	-0.12	0.24	III	...	...	III
2065....	III	-0.10	0.26	III	...	...	III
2100....	I	-0.56	0.16	I	...	0.10	I
2107....	IV	0.13	0.38	IV	<1	...	IV
2121....	VI	0.25	0.85	VI	...	0.7	VI
2134....	IV	-0.02	0.25	III	...	0.2	III-IV
2136....	III	-0.13	0.28	III	...	0.04	III
2154....	V	0.30	0.68	V	<2.5	...	V
2155....	VI	0.23	0.80	VI	...	...	VI
2156....	...	-0.07	0.12	III	...	0.06	III
2157....	...	-0.16	0.19	III	...	0.03	III
2164....	III	-0.24	0.10	II	...	0.05	II-III
2173....	V-VI	0.34	0.84	VI	...	...	VI
2193....	...	...	...	...	...	VI: <sup>d</sup>	VI(?)
2210....	VII	0.11	0.71	VII	...	...	VII
2213....	V-VI	0.28	0.70	V	2	...	V
2214....	II	-0.27	0.11	II	...	0.04	II
2231....	V	0.24	0.62	V	...	1.3	V
2257....	VII	...	...	...	old?	12 <sup>a</sup>	VII
H-2....	...	0.21	0.62	V	...	...	V
H-11....	VII	-0.02	0.62	VII	old	12	VII
Cl 132..	...	...	...	...	...	I:	I(?)

NOTE.—Age estimates in col. (7) are taken from Gascoigne (1980) for NGC 1466, 1835, 1868, 2231, 2257, and H11. See also Stryker (1981) for NGC 2257. The remaining ages are from Hodge (1981). Ages in cols. (6) and (7) are in units of  $10^9$  yr.

<sup>a</sup>Contains RR Lyrae variables (Graham 1973).

<sup>b</sup>Spectral type similar to NGC 1711, 1850, 1854, 1855, and 1953 (Ford 1970).

<sup>c</sup>Spectral type similar to NGC 2031, 2058, 2065, and other type III clusters (Ford 1970).

<sup>d</sup>Spectral type similar to other old clusters—type selected to be VI but very uncertain.

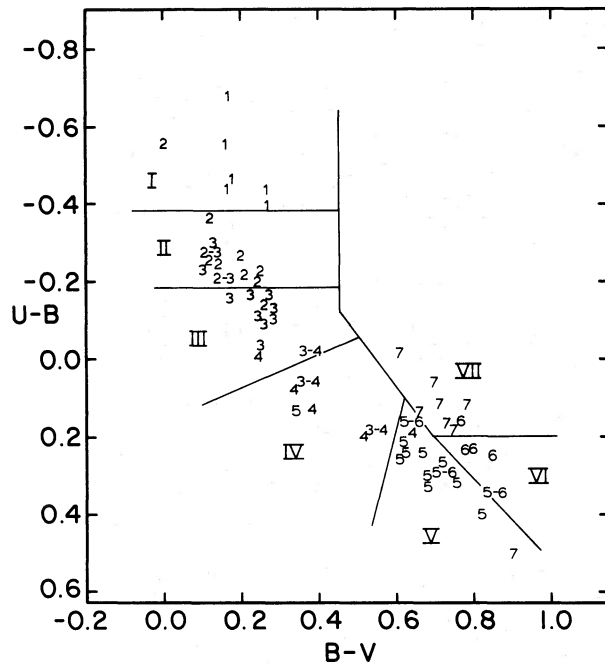


FIG. 3.—The two-color ( $U-B$ ) vs. ( $B-V$ ) distribution for the LMC clusters from Table 3 that have been classified by Searle, Wilkinson, and Bagnuolo (1980). The SWB classifications are indicated by denoting each point by its SWB class (1–7). Our boundaries between groups are shown. The correspondence between our classification and that of SWB is generally good; only a few discrepant points can be found.

The data required for the following discussion of the cluster velocities are collected in Table 4. The clusters are grouped into five main age classes, corresponding approximately to SWB types I–III, IV, V, VI, and VII, having (with considerable uncertainty—see Hodge 1981) ages  $\leq 10^9$ ,  $1-3 \times 10^9$ ,  $3-6 \times 10^9$ ,  $6-10 \times 10^9$ ,  $\geq 10^{10}$  yr (Frenk and Fall 1982), respectively. The adopted mean velocities of Table 2 are given in Table 4 in column (2), the gas or supergiant velocities in column (3), and their difference in column (4). The last three columns give, (col. [5]), the position angle in the plane of the sky about the H I rotation center at  $\alpha = 5^{\text{h}}21^{\text{m}}$ ,  $\delta = -69^{\circ}17'$ , (col. [6]), the radius from this center, and, (col. [7]), the galactocentric velocity for each cluster. The derivation of these data are discussed further in § V.

#### V. THE KINEMATICS OF THE CLUSTER POPULATION

Figure 4 shows, for each age class, the cluster velocity against the local H I disk velocity. From Figure 4 (*left*), we see that the young clusters (groups I–III) follow the disk velocities very closely, as we would expect (cf. Ford 1970), with a weighted mean difference  $\langle V_{\text{cl}} - V_{\text{HI}} \rangle = -11 \pm 5 \text{ km s}^{-1}$ , and with a dispersion of only  $12 \text{ km s}^{-1}$  after correction for measuring errors. The intrinsic dispersion and mean velocity difference are essen-

tially unchanged if the group IV clusters are included. The older clusters (groups V–VII) are shown in Figure 4 (*right*). The intrinsic dispersion is larger at  $23 \text{ km s}^{-1}$ , and the mean velocity of the older clusters is about  $25 \text{ km s}^{-1}$  less than the mean disk velocity, as discovered earlier by Ford (1970).

This  $25 \text{ km s}^{-1}$  difference is surprising, as is the fact that the intermediate age clusters (Groups V and VI) behave like old, rather than young, clusters. Before considering its implications, we should eliminate the possibility that the older cluster velocities are systematically in error. An obvious source of error is the presence of solar contamination of the spectra. We have discussed earlier a comparison of Searle and Smith's velocities with our own: the good agreement in the mean indicates that solar contamination is not the problem. Another check comes from Figure 5, which shows the difference  $\Delta V = (V_{\text{cl}} - V_{\text{disk}})$  for the older clusters against their mean surface brightness within a  $15''$  aperture (the photometry comes from Bernard and Bigay 1974 and Bernard 1975). If solar contamination were important, then it should affect most strongly the lowest surface brightness clusters; there is no sign in Figure 5 of such a dependence of velocity on surface brightness.

Is it possible that errors in the H I disk velocities are the cause of the systematic difference seen in Figure 4? This seems unlikely. Although the disk velocities are uncertain for a few clusters, for most they are not. And the well-behaved velocities of the young clusters make this explanation implausible.

Another possible source of systematic error comes from spectrograph zero-point problems, but again this seems unlikely here because the data we use come from five different spectrographs. In addition, the systematic difference between cluster and local disk velocities is seen only for the older clusters, and not for the blue clusters. We feel inclined, after this discussion, to accept the results of Figure 4 (*right*) as real, and to look for their explanation.

We noticed that the clusters with the most negative values of  $\Delta V = (V_{\text{cl}} - V_{\text{disk}})$  lie mainly in the western part of the LMC. Figure 6 shows  $\Delta V$  for the older clusters against their position angle. This position angle  $\theta$  in the plane of the sky is measured about the H I rotation center of the LMC,  $C_{\text{HI}}$ , at  $\alpha = 5^{\text{h}}21^{\text{m}}$ ,  $\delta = -69^{\circ}17'$ , from an unpublished rotation study by K. C. Freeman and D. Carrick. The position angle is zero to the north and increases to the east, as usual. From Figure 6, we see that the mean value of  $\langle V_{\text{cl}} - V_{\text{disk}} \rangle$  for the older clusters is about  $-10 \text{ km s}^{-1}$  for  $0^{\circ} \leq \theta \leq 160^{\circ}$  and about  $-40 \text{ km s}^{-1}$  for  $\theta \geq 200^{\circ}$ , with a dispersion of about  $20 \text{ km s}^{-1}$  in each case. For comparison, the young clusters are also shown in Figure 6: as we would expect from Figure 4 (*left*), they are clustered about  $\Delta V \sim 0$ , with no significant dependence on position angle. Figure 6 indicates that *the kinematics of the older*

TABLE 4  
CLUSTER VELOCITIES AND POSITIONS

NGC	$\frac{V_{C1}}{km\ s^{-1}}$	$\frac{V_{HI}}{km\ s^{-1}}$	$\frac{V_{C1}-V_{HI}}{km\ s^{-1}}$	P.A.	Radius	$\frac{V_{C1,c}}{km\ s^{-1}}$
(1)	(2)	(3)	(4)	(5)	(6)	(7)
(a) Groups I-III (Young)						
1711....	230±9	250	-20	251	2.7	16±9
1749....	308±17	275	33	291	2.6	93±17
1755....	257±16	275	-18	291	2.6	42±16
1774....	310±16	290	20	310	2.9	94±16
1805....	312±9	295	17	328	3.6	95±9
1810....	322±19	300	22	328	3.3	104±19
1818....	300±7	300	0	329	3.3	82±7
1850....	246±15	275 <sup>b</sup>	-29	293	1.2	28±15
1854....	242±9	270 <sup>d</sup>	-28	290	1.1	23±9
1866....	281±6	300	-19	348	3.9	60±6
1903....	262±15	260	2	260	0.3	42±15
1944....	270±22	250 <sup>b</sup>	20	178	3.2	51±22
2004....	309±11	305	4	25	2.2	85±11
2031....	242±26	240	2	149	2.0	19±26
2041....	268±17	300 <sup>d</sup>	-32	34	2.7	42±17
2058....	263±21	260	3	124	1.6	39±21
2065....	214±19	255	-41	125	1.7	-10±19
2100....	267±13	270 <sup>d</sup>	-3	89	1.9	41±13
2136....	238±16	245	-7	98	2.8	10±16
2156....	285±17	300	-15	80	3.4	56±17
2157....	276±8	... <sup>d</sup>	...	88	3.2	47±8
2164....	223±6	300 <sup>d</sup>	-27	82	3.5	43±6
2214....	289±10	300 <sup>b</sup>	-11	84	4.8	57±10
Cl 132..	272±16	275	-3	24	1.7	49±16
(b) Group IV						
1831....	253±13	295	-42	340	4.6	34±13
1856....	245±8	255 <sup>d</sup>	-10	276	1.0	27±8
1868....	260±30	300 <sup>b</sup>	-40	352	5.4	39±30
1872 <sup>a</sup> ...	261±50	255	6	263	0.7	42±50
1885....	282±19	260	22	298	0.6	62±19
1953....	267±11	270	-3	41	0.6	45±11
1987....	253±23	240	13	160	1.6	32±23
2107....	248±23	245	3	127	2.3	23±23
2134....	263±12	240 <sup>d</sup>	23	128	3.2	37±12
(c) Group V						
1644....	242±23	260	-18	302	5.1	31±23
1751....	196±16	245	-49	253	2.4	-19±16
1783....	277±9	295	-18	325	3.9	60±9
1806....	220±10	275 <sup>d</sup>	-55	304	2.1	3±10
1846....	236±12	295	-59	324	2.2	17±12
1917....	229±16	265	-36	329	0.3	8±16
2154....	264±13	290 <sup>b</sup>	-26	63	3.9	34±13
2213....	248±10	275	-27	124	4.8	19±10
2231....	270±24	... <sup>c</sup>	...	79	5.7	35±24
H-2.....	183±27	255	-72	211	0.5	-37±27
(d) Group VI						
1652....	241±40	255	-14	274	3.9	30±40
1978....	286±8	310	-24	14	3.1	62±8
2121....	219±15	235 <sup>d</sup>	-16	137	3.2	-6±15
2155....	284±15	290 <sup>d</sup>	-6	48	5.2	52±15
2173....	232±22	275 <sup>b</sup>	-43	145	4.8	7±22
2193....	265±28	280 <sup>b</sup>	-17	51	6.1	29±28
(e) Group VII						
1466....	196±12	245 <sup>b</sup>	-49	242	8.3	-2±12
1754....	227±9	260	-33	239	2.6	12±9
1786....	265±7	280	-15	304	2.5	49±7
1835....	204±4	260	-56	262	1.4	-13±4
1841 <sup>a</sup> ...	288±37	... <sup>c</sup>	...	183	14.8	84±37
1898....	181±15	255	-74	222	0.5	-39±15
2019....	275±8	260	15	134	1.3	52±8
2210....	313±10	290 <sup>d</sup>	23	86	4.5	82±10
2257....	284±19	... <sup>c</sup>	...	61	8.5	45±19
H-11....	249±16	260 <sup>b</sup>	-11	103	4.7	18±16

NOTE.—Data in col. (2) are  $\langle V \rangle$  from Table 2, col. (10). Position angle and radius are based on coordinates of Shapley and Lindsay (1963) and Sulentic and Tifft (1973). Center at  $\alpha = 5^h 20^m 9$  and  $\delta = -69^\circ 17' 6$  (1975). P.A. defined E from N. N-S is P.A.  $0^\circ$ .

<sup>a</sup>NGC 1872 and NGC 1841 are tabulated but not used in the analysis: NGC 1872 because of its large uncertainty  $\Delta V$ ; NGC 1841 because of its large radius from the LMC center.

<sup>b</sup>Uncertain  $V_{HI}$ : extrapolation beyond H I.

<sup>c</sup>Uncertain  $V_{HI}$ : far beyond H I, extrapolation impossible.

<sup>d</sup>Uncertain  $V_{HI}$ : complex H I velocity structure.

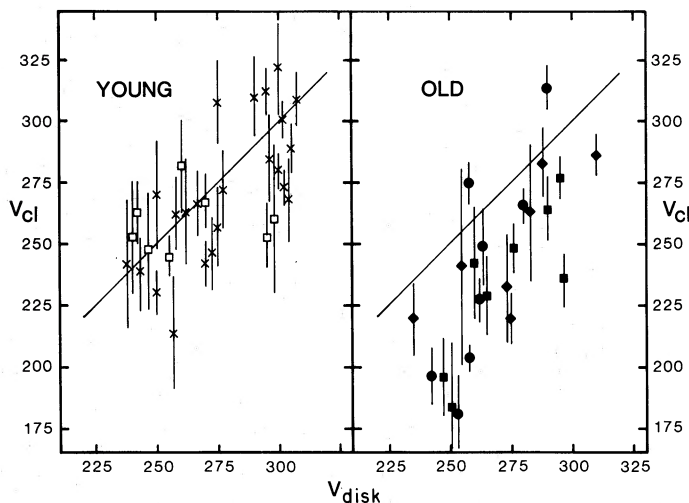


FIG. 4.—(left) The observed cluster velocity  $V_{cl}$  in  $\text{km s}^{-1}$  from Table 4 for the young clusters (groups I–III, indicated by crosses) compared to the disk (H I, H II, or supergiant) velocity at each cluster's position. Equality is indicated by the line of slope unity. The intermediate age ( $\sim 10^9$  yr) group IV clusters are shown as unfilled squares. The young clusters and the gas in their vicinity have very similar velocities. (right) As for Fig. 4 (left), but for the older clusters, groups V, VI, and VII, indicated by filled squares, diamonds, and circles, respectively. The systematic offset to lower velocities is real and significant.

clusters are less disorderly than they at first appeared to be, and further investigation seems worthwhile.

We now attempt a rotation solution for the system of older clusters. First, it is necessary to transform the observed heliocentric cluster velocities to galactocentric velocities, because galactic rotation produces an apparent heliocentric velocity gradient of about  $40 \text{ km s}^{-1}$  over the region of the LMC in which our clusters are found. For consistency with the radial velocity compilation of Feitzinger and Weiss (1979), we use their transformation to galactocentric velocities (this transfor-

mation corrects for galactic rotation of  $250 \text{ km s}^{-1}$  and the standard solar motion). The galactocentric velocities  $V_{cl,c}$  are given in column (7) of Table 4. Figure 7 shows the velocities  $V_{cl,c}$  of the older clusters against their position angle,  $\theta$ , as defined above. There is obviously a fair amount of ordered motion, and there is no obvious kinematic difference between our three subclasses (V, VI, and VII).

Before investigating the rotation solutions we need to discuss whether the outlying clusters NGC 1466, NGC 1841, and NGC 2257 are to be included. These clusters

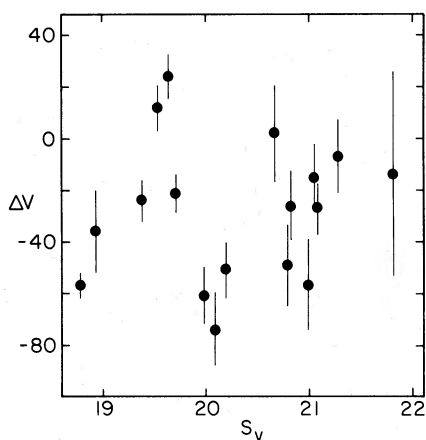


FIG. 5.— $\Delta V = V_{cl} - V_{disk}$  in  $\text{km s}^{-1}$  from Table 4 vs. mean  $V$ -band surface brightness  $S_V$  (in  $\text{mag arc sec}^{-2}$ ) within a  $15''$  aperture from Bernard and Bigay (1974) and Bernard (1975). No trend of  $\Delta V$  with  $S_V$  is seen.

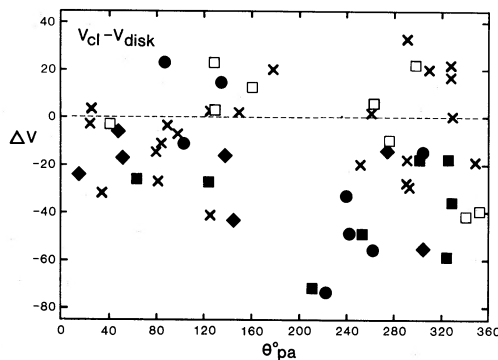


FIG. 6.— $\Delta V = V_{cl} - V_{disk}$  in  $\text{km s}^{-1}$  from Table 4 vs. position angle  $\theta_{pa}$  in degrees in the plane of the sky and about the rotation center  $C_{H I}$ . The symbols are as Fig. 4 (filled—older clusters; crosses—young; unfilled—intermediate). While there is no apparent trend in  $\Delta V$  with  $\theta$  for the younger clusters, a trend can be seen for the older clusters.

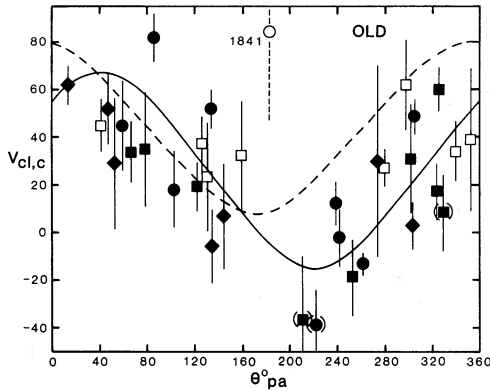


FIG. 7.—Galactocentric cluster velocities  $V_{cl,c}$  in  $\text{km s}^{-1}$  from Table 4 vs. position angle  $\theta_{pa}$  in the plane of the sky. Groups IV (unfilled), and V–VII (filled) are shown. The position of NGC 1841 (Group VII) is indicated; NGC 1841 has been excluded from the rotation solutions. The best fit solution (3) from Table 5 for the 25 older Group V–VII clusters is shown as the continuous line. The dashed line is the rotation solution for the H I and the youngest clusters (Table 5, solution 1). The intermediate-age Group IV clusters are not included in either solution, but are shown for comparison with the older clusters. Clusters within radius  $r \leq 0.5$  from  $C_{H\text{I}}$  are enclosed in parentheses.

lie  $8^{\circ}3$ ,  $14^{\circ}8$ , and  $8^{\circ}5$ , respectively, from the center of the LMC. It appears from Figure 7 (see also Figure 10 later) that NGC 1466 and NGC 2257 are associated with the LMC and, as we shall see, are consistent with being in circular orbits about it (but see Cowley and Hartwick 1981*b*). We include these clusters in our analysis. The relationship of NGC 1841 to the LMC is much more uncertain. While its velocity is within  $\sim 50 \text{ km s}^{-1}$  of the systemic velocity of the LMC, it does not appear to share the same kinematical properties as the remaining clusters in Figure 7. While such circular arguments are unsatisfactory, it is this, combined in particular with the great separation of NGC 1841 from the LMC ( $15^{\circ}$ ), that led us to reject it from the rotation solutions that follow.

In a full rotation analysis, we would solve for the shape and amplitude of the mean rotation curve for the cluster system, the inclination of the mean plane of the system, and the position angle of the line of nodes (i.e., the line of intersection of the plane of the system and the plane of the sky). In addition, Magellanic spirals like the LMC are asymmetric and their rotation centers do not usually coincide with any identifiable structural feature (de Vaucouleurs and Freeman 1973), so we would also need to solve for the rotation center. Such a full solution is obviously out of the question with only 25 “old” clusters in our sample, so we must make some assumptions.

We assume that the inclination,  $i$ , of the mean plane of the older cluster system is  $27^{\circ}$ , in agreement with the

inclination determined from the large-scale structure of the LMC itself (see de Vaucouleurs and Freeman 1973). We assume also that the rotation center for the older cluster system is the same as the rotation center  $C_{H\text{I}}$  for the H I, as defined above. The line of nodes for the older clusters appears to differ (Fig. 7) from the kinematically determined line of nodes for the H I component of the LMC (in position angle  $171^{\circ}$ ; Freeman and Carrick 1969), which is similar to that derived from optical velocities and isophotes (de Vaucouleurs and Freeman 1973). Therefore we must solve for the position angle of the line of nodes for the older cluster system: if we were to assume that its line of nodes were similar to the line of nodes for the H I, then we would obviously derive a misleadingly large value for the velocity dispersion of the older cluster system. For simplicity we assume, following Frenk and White (1980), that the mean rotational velocity of the cluster system is independent of distance from the rotation center,  $C_{H\text{I}}$  (i.e., a “flat” rotation curve—this assumption can be checked later, as can the assumption  $i = 27^{\circ}$ ).

Given these assumptions the rotation solution to be fit by minimizing residuals in the  $V_{cl,c}$  data of Table 4 is

$$V(\theta) = V_m \left\{ \left[ \tan(\theta + \theta_0) \sec i \right]^2 + 1 \right\}^{-0.5} + V_0;$$

$$0 \leq \theta \leq 2\pi,$$

where  $V(\theta)$  is the rotational velocity projected into the line of sight, and  $\theta$  is the position angle as defined previously. The inclination  $i = 27^{\circ}$ . A three-parameter nonlinear  $\chi^2$ -minimization routine was used (see, e.g., Bevington 1969), the free parameters being the position angle of the line of nodes  $\theta_0$ , the amplitude of the rotation solution  $V_m$ , and the systemic velocity  $V_0$ .

A variety of solutions were determined for subsets of the data in Table 4. These solutions are tabulated in Table 5, with the subset used being given in column (2), the number of clusters in column (3), the solutions for  $\theta_0$ ,  $V_m$ , and  $V_0$  with errors for each in columns (4), (5), and (6), respectively, and the intrinsic dispersion about the fit, after correction for the uncertainties in  $V_{cl,c}$ , being given in column (7). The rotation solutions in Table 5 hold some real surprises, primarily for the older clusters. We will return to these after discussing the solution for the youngest clusters.

The solution derived for the youngest clusters should compare well with that found for the gas. We would expect these to be similar, and they are. The H I and H II rotation solution for gas at radii  $r \geq 1^{\circ}$  from the rotation center is the first entry in Table 5, followed by that derived here for the young clusters, our groups I–III.  $V_m$  and  $V_0$  are the same to within  $1 \sigma$  ( $3\text{--}5 \text{ km s}^{-1}$ ) in the uncertainty, while the position angle,  $\theta_0$ , of the line of nodes differs by less than  $2 \sigma$  (since the

TABLE 5  
ROTATION SOLUTIONS

Solution (1)	Groups (2)	$N_{cl}$ (3)	$\theta_0$ (degrees) (4)	$V_m$ ( $\text{km s}^{-1}$ ) (5)	$V_0$ ( $\text{km s}^{-1}$ ) (6)	$\sigma_i$ ( $\text{km s}^{-1}$ ) (7)
(1) .....	H I/H II <sup>a</sup>	...	171	36	44	...
(2) .....	I-III	24	$1 \pm 5$	$37 \pm 5$	$40 \pm 3$	15
(3) .....	V-VII <sup>b</sup>	25	$41 \pm 5$	$41 \pm 4$	$26 \pm 2$	$17^c$
(4) .....	V-VII <sup>d</sup>	25	$43 \pm 5$	$43 \pm 4$	$26 \pm 2$	18
(5) .....	V-VII <sup>e</sup>	22	$42 \pm 5$	$40 \pm 4$	$27 \pm 2$	17
(6) .....	IV-VII	33	$41 \pm 5$	$37 \pm 3$	$27 \pm 2$	17
(7) .....	IV-V	18	$31 \pm 11$	$22 \pm 7$	$25 \pm 4$	13
(8) .....	VI-VII	15	$45 \pm 6$	$43 \pm 4$	$31 \pm 3$	17
(9) .....	VII <sup>f</sup>	9	$44 \pm 6$	$54 \pm 7$	$38 \pm 4$	16
(10) .....	V-VII	25	$1^g$	$30 \pm 4$	$18 \pm 2$	26
(2') .....	I-III	24	$161 \pm 5$	$42 \pm 4$	$37 \pm 3$	16
(3') .....	V-VII	25	$18 \pm 5$	$33 \pm 4$	$22 \pm 2$	22
(9') .....	VII <sup>f</sup>	9	$34 \pm 7$	$38 \pm 4$	$33 \pm 4$	22

NOTES.—Position angle (col. [4]) is defined east of north. N-S is PA  $0^\circ$ . All solutions except (1) are derived from a three parameter ( $\theta_0, V_m, V_0$ ) rotation solution fit (see text) to the data of Table 4, col. (7). All solutions are for  $i = 27^\circ$  (except 4). Solutions (2'), (3'), and (9') are as (2), (3), and (9) but using velocities corrected for a transverse motion of the LMC towards the east (P.A.  $90^\circ$ ) with a velocity of  $300 \text{ km s}^{-1}$  (see text).

<sup>a</sup>H I solution from Freeman and Carrick (1969). See also Smith and Weedman (1971). Adopted “young” solution shown in Figs. 7, 8, and 9.

<sup>b</sup>Adopted “old” solution shown in Figs. 7, 8, and 9.

<sup>c</sup> $\sigma_i = 18 \text{ km s}^{-1}$  about this fit for the group VII clusters alone; compare with solution (9).

<sup>d</sup>Solution for  $i = 45^\circ$ , not  $27^\circ$ .

<sup>e</sup>Solution omitting three clusters having  $r \leq 0.5$ —see Table 4.

<sup>f</sup>There are only nine objects in these solutions (see text)!

<sup>g</sup> $\theta_0$  constrained to be the same as found for the young clusters in solution (3).

uncertainty in  $\theta_0$  for the H I and H II solutions is probably  $\pm 3^\circ$ – $5^\circ$ ). The velocities  $V_{cl,c}$  for the young clusters are plotted in Figure 8 against position angle  $\theta$ .

This consistency is encouraging and suggests again that our adopted blue cluster velocities are not subject to serious systematic biases.

Since the youngest clusters give a rotation solution consistent with that from the H I and H II studies, we have adopted this latter, better determined solution as the “young” solution, plotted it in Figure 8, and repeated it in Figures 7 and 9.

While the solution for the youngest clusters held no real surprises, the same is not true of that for the older clusters. For solution (3), that for groups V, VI, and VII, we see that the amplitude of the rotation,  $V_m = 41 \pm 4 \text{ km s}^{-1}$ , is essentially identical to that for the youngest clusters for which  $V_m = 37 \pm 5 \text{ km s}^{-1}$ , as is the intrinsic dispersion. This solution, our “old” solution, shown in Figure 7 and repeated in Figures 8 and 9, suggests that the older clusters (and in this subset we include the very oldest group VII clusters) form a rapidly rotating disk-like system.

This in itself is not so surprising: most of these clusters are probably just older examples of the blue clusters which are kinematically similar to the H I/H II disk. The striking and surprising feature of solution (3) is that the systemic velocity, and the position angle of the line of nodes for the older cluster system and the gas, are very significantly different; in particular, the lines of nodes differ by  $50^\circ$ !

Before discussing this rather radical result, we need to test the assumptions involved in the rotation solution and look more closely at the older cluster data. First, we tried rotation solutions for the same group V, VI, and VII clusters with  $i = 60^\circ$  and  $45^\circ$ , instead of  $i = 27^\circ$ . The differences were within the uncertainty of the fit for  $i = 27^\circ$ . The  $i = 45^\circ$  solution is given in Table 5 (solution [4]). One would clearly not try to determine  $i$  by this procedure! Another possible problem was the inclusion of clusters having  $r \leq 0.5$  (indicated by parentheses in Fig. 7). Although the  $V \approx \text{constant}$  rotation curve is not a good approximation so close to  $C_{H I}$ , solution (5) showed that the inclusion of these clusters introduced no significant bias. Clusters in group IV, those with ages

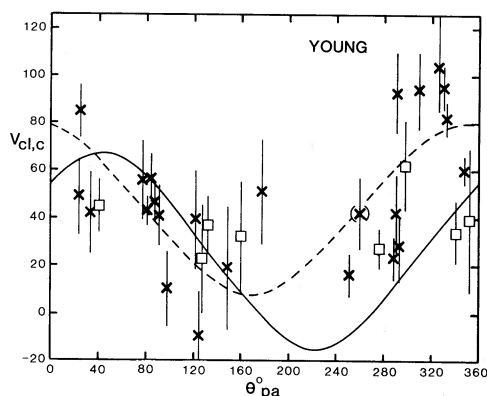


FIG. 8.—As for Fig. 7, but for the young clusters (Groups I–III; crosses). The young (dashed) and old (continuous) solutions are as discussed in Fig. 7. The intermediate age clusters (unfilled squares) are again shown only for comparison with the young clusters. They are not included in either rotation solution. Parentheses indicate clusters with  $r \leq 0.5$ .

around  $10^9$  yr, were added to the older groups in solution (6) but with minimal effect. It is interesting to note that a solution with groups IV and V alone (solution [7]) gave a value of  $\theta_0$  intermediate between that for the young clusters, groups I–III, in solution (2), and the oldest, groups VI and VII, in solution (8). The significance of this result is not high, however.

There is a real possibility that the Magellanic Clouds have a transverse motion of about  $300 \text{ km s}^{-1}$  to the east, i.e. toward P.A.  $90^\circ$  (Mathewson, Schwarz, and Murray 1977; Feitzinger, Isserstedt, and Schmidt-Kaler 1977; Lin and Lynden-Bell 1982). Because of the large angular extent of the LMC, this would produce an apparent solid body motion across the LMC which would affect our rotation solutions. We would not expect the differences between the “young” and “old” solutions of Table 5 to disappear, however, because the distributions of these clusters over the LMC are so similar (Fig. 1). We have made rotation solutions, including this translation, for the young (I–III), old (V–VII), and oldest (VII) clusters. The solutions appear as 2', 3', and 9' in Table 5. As expected, the main effect of the translation is to move the position angle of the kinematic line of nodes by about  $20^\circ$ . However, the significant differences remain between the systemic velocity and line of nodes for the older clusters and the young clusters. We note also that the velocity dispersions for these solutions are consistently larger than for the corresponding solutions without the translation.

This brings us to the particularly interesting results of solution (9), that for the oldest (group VII) clusters in the LMC. These clusters are thought to share the population and age characteristics of globular clusters in our own Galaxy (e.g., Stryker 1981) and are therefore those most likely to have halo kinematics (i.e., little rotation, high  $z$  velocity dispersion). While there are only nine of

these clusters, it is fascinating to note that solution (9) indicates that these clusters also form a flattened disk-like component. This is apparent also from Figure 7. In fact their dispersion about the standard “old” solution in Figure 7 (solution [3]) is only  $18 \text{ km s}^{-1}$ . These solutions suggest that there is no old, kinematical halo population among the clusters of the LMC. This result is not strongly coupled to the difference in the line of nodes for the old and young clusters. Constraining the line of nodes for the group V–VII clusters to be that of the young clusters<sup>6</sup>, i.e.,  $1^\circ$ , results in a velocity dispersion (Table 5, solution [10]) for the older clusters that is still small, although significantly larger than for the full rotation solution (compare solutions [3] and [10] in Table 5).

We will return to this question again in § VI, along with the discussion of the implications of the large difference in the line of nodes between the “young” and “old” cluster populations. Meanwhile, we will complete our discussion of the kinematics of the clusters.

Most of the kinematical data available for the LMC (see Feitzinger and Weiss 1979) are for the young population: the data we have presented in Figure 7 for the older clusters are the only kinematical information pertaining to a population that is definitely not young. It seems useful to compare the kinematics of the older clusters with those of the planetary nebulae, even though the planetaries probably include objects with a wide range of ages and masses, from about 1 to  $3.5 M_\odot$  (Wood and Cahn 1977; Wood 1981). Figure 9 shows the  $V_{\text{pl,c}}-\theta$  data for the planetaries: the galactocentric velocities come from Feitzinger and Weiss (1979). The planetaries do appear to show a wide range of kinematical properties. As noted by Smith and Weedman (1972), the planetaries within about  $2^\circ$  of the rotation center follow the H I/H II region rotation curve fairly closely. Several of the outer planetaries are also close to this rotation curve. However, at least two of them lie near the older cluster rotation curve, and three of them are far from either curve, near  $V = 60 \text{ km s}^{-1}$  and  $120^\circ < \theta < 220^\circ$ . Two of the three have velocities close to the local H I velocity, which is, however, significantly different from the expected mean rotational velocity as calculated from the H I/H II rotation curve. This range in kinematical behavior probably results from the wide range in age of the planetaries; also inhomogeneous and asymmetric planetary nebula shells could lead to a few discrepant velocities.

It would be reassuring to have independent observational evidence about the kinematical properties of the old disk. The data presented here for the old clusters are all that are available so far, since the planetary data

<sup>6</sup>This is an unjustified constraint since, as mentioned earlier in this section, the older clusters show systematic velocity differences when compared in the  $\Delta V(\theta)$  plane (Fig. 6) to the younger group I–III clusters.

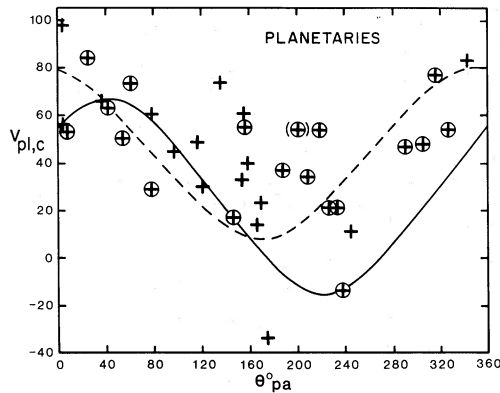


FIG. 9.—Galactocentric planetary nebula velocities  $V_{pl,c}$  in  $\text{km s}^{-1}$  from Feitzinger and Weiss (1979) vs. position angle  $\theta_{pa}$ . Those circled have  $r < 2^\circ$ . Parentheses indicate planetaries having  $r < 0.5$ . The planetaries tend to lie near the young solution, but the scatter is large. The rotation solutions are from Figs. 7 and 8.

were inconclusive. Kinematical observations of the long-period variables and carbon stars would be very valuable in the context.

Finally we return to Figure 7, to check whether there is any systematic radial trend of the velocity residuals from the mean rotation curve. A trend would mean that our assumption of constant mean rotational velocity for the older cluster system is not adequate. Figure 10 shows  $\Delta V = k[V_{cl,c} - V_{fit}(\theta)]$  against radius  $r$ .  $r$  is the apparent distance (in the plane of the sky) from the rotation center  $C_{H1}$ ,  $V_{fit}(\theta)$  is the fitted rotation solution velocity (solution [3]; the continuous curve in Figure 7), while  $k = -1$  for  $131^\circ < \theta < 311^\circ$ , and  $k = +1$  elsewhere. Clusters with negative  $\Delta V$  have velocities closer to  $V_{systemic}$  than expected for a flat rotation curve. Clusters within  $25^\circ$  of the minor axis are distinguished in Figure 10 by parentheses. Since we expect  $\Delta V \sim 0$  for

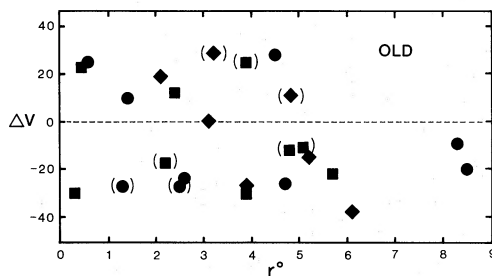


FIG. 10.— $\Delta V = k[V_{cl,c} - V_{fit}(\theta)]$  against radius  $r$  in degrees from the rotation center  $C_{H1}$  for the older clusters (Groups V–VII).  $V_{fit}(\theta)$  is solution (3) from Table 5, i.e., that shown by a continuous line in Figs. 7–9.  $k = -1$  for  $131^\circ \leq \theta_{pa} \leq 311^\circ$ , and  $k = +1$  otherwise. Clusters having  $\theta_{pa}$  within  $\pm 25^\circ$  of that of the minor axis are enclosed in parentheses. The sense of  $\Delta V$  is such that clusters with  $\Delta V < 0$  fall below a flat rotation curve, i.e., they have velocities closer to the systemic velocity. Typical uncertainties for these  $\Delta V$  values are  $\pm 10$ – $20 \text{ km s}^{-1}$ .

clusters on or near the minor axis, these clusters contribute little to the question being investigated here. In this plane, any systematic deviation from constant mean rotation will show up as a trend of  $\Delta V$  with  $r$ . For  $r \leq 5^\circ$  there is no significant trend, nor is there any significant difference in the residuals for our three subclasses (the uncertainties on these  $\Delta V$  values are typically  $\pm 10$ – $20 \text{ km s}^{-1}$ ). The two clusters NGC 1466 and NGC 2257, which lie on opposite sides of the LMC near  $r \sim 8.5$ , have negative residuals, which suggests that the true mean rotation curve may fall slightly between  $r \sim 5^\circ$  and  $r \sim 9^\circ$ , as one would expect for an exponential disk of constant  $M/L$  ratio (see Freeman 1970). We can conclude from Figure 10 that the assumption of constant mean rotational velocity is adequate, certainly out to  $r \sim 5^\circ$ , and probably out to  $r \sim 9^\circ$ .

## VI. DISCUSSION

Our data present us with two novel results. First, even the oldest globular clusters in the LMC appear to have disk kinematics. Second, the rotation solutions for the gas and young clusters differ very significantly from that for the older clusters, not in amplitude, but in the systemic velocity and in the position angle of the apparent line of nodes. We will discuss this latter result first. The obvious questions are: what do the observed differences imply for the structure of the LMC, and how can these differences arise?

In simple kinematic terms, if we assume that the gas and clusters are moving in circular orbits, the difference in the position angles of the line-of-nodes would suggest that we are viewing two disks, superposed along the line of sight, but with rotation axes that differ by  $\sim 50^\circ$ ! While the difference in systemic velocity may indicate that these disks are physically separated from one another, the appearance of the LMC would suggest that the gas, the younger clusters, and the older clusters all move in a common gravitational potential. The similarity in velocity dispersions and rotational velocities (Table 5) would also suggest that both the young and old systems have similar inclinations.

A problem with such a picture is that two coincident disks with different orientations are not stable; alignment of the rotation axes will tend to occur, typically on time scales of several rotation periods (Hunter and Toomre 1969 and Tubbs and Sanders 1979; note that  $t_{rot} \sim 2 \times 10^8 \text{ yr}$  at  $r \sim 3^\circ$  for  $V_{rot} \sim 80 \text{ km s}^{-1} = 36/\sin 27^\circ$ ). In such a realignment, gas will settle dissipatively to a new disk. This is not the case, however, for any nondissipative stellar component. The main effect of the realigning torques will be to increase the velocity dispersion of the stellar component. If this two-disk picture is appropriate for the LMC, then clearly such structure has only existed for a relatively short time ( $\leq 10^9 \text{ yr}$ ). This would suggest that the older clusters,

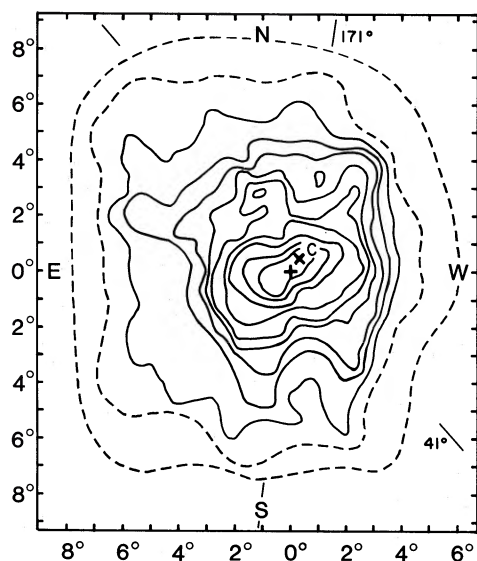


FIG. 11.—Red, R band, isophotes for the LMC from de Vaucouleurs (1957). The photometric center is indicated by a plus symbol. The rotation center  $C_{H1}$  is shown as C. The photometric and kinematic major axis in position angle  $171^\circ$  from de Vaucouleurs (1957) and de Vaucouleurs and Freeman (1973) is shown. The line of nodes found for the older clusters in position angle  $41^\circ$  is indicated also. The outermost continuum isophote is at  $R \sim 24.1$  mag arcsec $^{-2}$ . The bar dominates the innermost isophotes.

which have all made  $\geq 10$  revolutions about the LMC, define the form of the gravitational potential in the LMC, and that the gas has been disturbed in some way. The motions of the young clusters reflect that of the gas from which they were born. Since group III–IV clusters with ages  $\sim 10^9$  yr still appear to have velocities very similar to the gas locally, a dynamical time for evolution of this system appears to be of this order.

The kinematic line of nodes for the older cluster system is in position angle  $40^\circ$ : does this then correspond in any way to the structural properties of the old population of the LMC? The standard line of nodes for the LMC is in position angle  $171^\circ$  (see Table 1 of de Vaucouleurs and Freeman 1973). This is also the kinematic line of nodes for the gas, and it comes mainly from the kinematics and distribution of young objects. It is interesting to look at the red-light isophotes of the LMC (Fig. 11, adopted from de Vaucouleurs 1957). Within  $5^\circ$  of the rotation center, where most of the older clusters lie, the isophotes are quite irregular. There is no clear elongation in position angle  $40^\circ$ . However, when the effects of visible Population I structures are taken into account, there may be a tendency for the red-light isophotes to be elongated away from position angle  $171^\circ$  toward position angle  $40^\circ$ . The photometric data are ambiguous, as are the planetary-nebula kinematical data discussed in § IV. This leaves us with little supporting

evidence for the contention that the older cluster parameters  $V_m$ ,  $V_0$ , and  $\theta_0$  are characteristic of the underlying older population, though dynamical arguments would suggest this to be the most likely situation.<sup>7</sup> If we take this to be the case, why then are the properties of the velocity field of the young population (i.e., the gas primarily) so different?

The kinematics of the gas will be affected by the interaction of the LMC with the gas of the LMC-SMC-Galaxy system, which may include the gaseous halo of the Galaxy (Mathewson and Schwarz 1976); direct observational evidence comes from the H I observations by Mathewson *et al.* (1979) of the entire area between the Magellanic Clouds. They report a continuous H I velocity field between the two clouds, which blends smoothly into the velocity field of the LMC itself and the Magellanic Stream. Further evidence for interaction comes from the sharp H I surface density gradient to the east of the LMC. We should also mention the double-valued H I velocity field observed to the east of the bar by McGee and Milton (1966).

It is difficult to assess the dynamical state of the gas, because we do not know how much these interactions affect the observed H I velocities. In addition, we cannot be sure that the H I velocity field is showing mainly circular motion in the gravitational field of the LMC. The apparent line of nodes for the gas could be significantly affected by internal streaming in the asymmetrical potential field of the LMC, by large-scale warping and distortion of the gas layer, and by external interaction in the LMC-SMC-Galaxy system. We should emphasize, however, that both the older population and the young population of the LMC are relatively cold. To produce the observed velocity field differences, it will be necessary to invoke processes that specifically affect the gaseous component. Detailed dynamical modelling will be needed to understand this situation.

Our very tentative picture of the structure of the LMC can be summarized as follows. The older populations of the LMC (age  $\geq 10^9$  yr) are characterized by the kinematics of the old (groups V–VII) clusters. The younger material, e.g., the gas, stars, and clusters, moves in the potential of the older populations. However, the gas motions are quite different from those of the older populations, and these motions are reflected in the kinematics of the young stellar objects, having ages comparable to or less than the dynamical time for evolution of this structure ( $\leq 10^9$  yr). The observed kinematical difference could be due to differences in the orientation of the gas and older populations (the two-disk

<sup>7</sup>Part of this difference between the kinematic line of nodes and the apparent elongation of the isophotes may be due to the transverse motion mentioned previously. A transverse motion of  $300 \text{ km s}^{-1}$  toward P.A.  $90$  is in the right sense to lessen the discrepancy—see Table 5 and Feitzinger, Isserstedt, and Schmidt-Kaler 1977.

model), or due to strong noncircular motions in the gas in the older population plane leading to an apparent change in the line of nodes. Interaction with gas external to the LMC may drive these motions.

The structure of the LMC is very clearly an enigma. Some useful theoretical and observational tests can be made that may help to resolve this problem. First, a closer look at the time scales for kinematical evolution of the young stellar objects away from strict correspondence with the gas motions may be valuable; e.g., the time scales for this may be much shorter if gaseous noncircular motions occur in the same plane as the older objects, than if planes of different orientation are involved. Observationally, radial velocities for long-period variables or any other obvious intermediate-age or old component, or surface photometry and star counts, where the young and old components are distinguished, would all be useful.

As we have noted previously, the oldest clusters appear to form a quite flattened disklike system. We can quantify this statement. The intrinsic velocity dispersion  $\sigma_i$  of the oldest clusters about the old solution, (3), of Table 5 is only  $18 \text{ km s}^{-1}$ . This is small compared to the rotational velocity in the plane of the LMC, i.e.,  $V_{\text{max}} \sim 80 \text{ km s}^{-1}$ , taking  $V_m = 36 \text{ km s}^{-1}$  from Table 5, and  $i = 27^\circ$ . If  $i = 27^\circ$ , a significant fraction of the observed  $\sigma$  should be the velocity dispersion out of the plane,  $\sigma_z$ . Conservatively, let us take  $\sigma_z = \sigma_i \approx 18 \text{ km s}^{-1}$ , leading us to overestimate the scale height and thereby underestimate the flattening. The procedure for estimating the scale height for such a population in the LMC potential is straightforward. The LMC H I rotation curve (Freeman and Carrick 1969) can be fitted by that expected for a self-gravitating constant  $M/L$  exponential disk (the rotation data cover too few scale lengths for questions concerning  $M/L$  variations to be answered). Assuming an exponential disk of scale length  $\alpha^{-1} \sim 1.6 \text{ kpc}$  for the LMC (at a distance of 55 kpc), and a  $z$  density distribution (van der Kruit and Searle 1981),

$$\rho(z) = \rho(0) \text{sech}^2(z/z_0),$$

we derive  $z_0 = 0.5 \text{ kpc}$  for  $r = 2\alpha^{-1} \sim 3.2 \text{ kpc}$  and  $V_{\text{max}} = 80 \text{ km s}^{-1}$ . At large  $z$  ( $z \gg z_0$ ),  $\rho(z)$  is well approximated by an exponential of scale height  $z_0/2$ , whereas for  $z \ll z_0$ ,  $\rho(z)$  reduces to a Gaussian distribution of dispersion  $z_0/\sqrt{2}$  (van der Kruit and Searle 1981). At  $z \approx z_0$ ,  $\rho(z)$  can usefully be considered to be exponential with scale height  $z_0$ . For  $\sigma_z = 16 \text{ km s}^{-1}$ , as in solution (9),  $z_0$  is only  $0.4 \text{ kpc}$ , increasing to  $0.7 \text{ kpc}$  for  $\sigma_z = 22 \text{ km s}^{-1}$ , and  $1.0 \text{ kpc}$  for  $\sigma_z = 26 \text{ km s}^{-1}$ . The clusters clearly form a quite flattened system.

Confirmation of this result will be difficult. The cluster sample cannot be increased easily, if at all. Radial velocities for other members of the oldest stellar popula-

tion (e.g., RR Lyrae stars) in the LMC will be extremely difficult to determine. Velocities with uncertainties  $\leq 15 \text{ km s}^{-1}$  are required.

Interestingly, Geisler and Hodge (1980) suggested that the high average ellipticity found by them for the old LMC clusters was due to their being disk, rather than halo, clusters, and as such formed from gas having higher specific angular momentum. However, the mean ellipticity for the oldest clusters in the LMC does not appear to be significantly different from that of the galactic globular clusters in a recent study by Frenk and Fall (1982).

The formation history of the globular clusters in the LMC and the Galaxy were then quite different. While the galactic globular clusters are all part of the halo population and probably preceded disk formation, the clusters of the LMC did not form until the disk itself was established. The presence in the LMC disk of the halo-type clusters with horizontal branches is not inconsistent with this picture: it simply means that the oldest clusters in the LMC are indeed very old and have abundances significantly lower than the present mean abundance of the old disk.

The possibility of a *stellar* halo in the LMC (i.e., no globular clusters) remains and is well worth investigation. It would be very interesting if the LMC turns out to have no stellar halo at all. We would then need to know why all star formation (and not just globular cluster formation) was inhibited during the LMC's collapse to the disk.

## VII. CONCLUSIONS

1. Velocities have been measured for 35 LMC globular clusters, which, when combined with data from other sources, give mean velocities for a total of 59 clusters ranging in age from  $\sim 10^8$  to  $\sim 10^{10}$  yr. These mean velocities have uncertainties that are typically  $10\text{--}20 \text{ km s}^{-1}$ , though nearly 10% still have quite poorly determined velocities with uncertainties of  $30\text{--}40 \text{ km s}^{-1}$ .

2. The clusters were age-grouped by SWB classes, supplemented by classification in the two-color  $U-B$ ,  $B-V$  plane for clusters not studied by SWB. Rotation solutions were made for two subsets of the clusters, those less than  $\sim 10^9$  yr old (SWB groups I-III) and those older than  $\sim 1\text{--}2 \times 10^9$  yr (SWB groups V-VII).

3. The youngest clusters were found, as expected, to have motions similar to that of the gas in their vicinity. They form a flattened disklike system having an amplitude for their rotation of  $37 \pm 5 \text{ km s}^{-1}$ , a galactocentric systemic velocity of  $40 \pm 3 \text{ km s}^{-1}$  and a line of nodes at P.A.  $1^\circ \pm 5^\circ$ , all quite consistent with the H I and H II region values of  $36 \text{ km s}^{-1}$ ,  $44 \text{ km s}^{-1}$ , and  $171^\circ$ , respectively. Their intrinsic line-of-sight dispersion is only  $15 \text{ km s}^{-1}$ .

4. The older clusters, not unexpectedly, were also found to lie in a flattened disklike system with a low line-of-sight dispersion of  $17 \text{ km s}^{-1}$  and a rotation amplitude of  $41 \pm 4 \text{ km s}^{-1}$ . What was unexpected was that both the line of nodes of this system at  $41^\circ \pm 5^\circ$  and the galactocentric systemic velocity at  $26 \pm 2 \text{ km s}^{-1}$  were found to be significantly different from those for the gas and the young clusters. If the motions of the older clusters characterize the old stellar population of the LMC, then the gas must be disturbed, acquiring (or appearing to do so) in the process a rotation axis tilted  $50^\circ$  from that of the older populations. The young cluster motions reflect the gas motions. The structure of the LMC is an enigma. Further observations are suggested.

5. The oldest nine clusters, those in SWB group VII, also appear to lie in a highly flattened disklike system. In fact, for a velocity dispersion  $\sigma_z$  of  $18 \text{ km s}^{-1}$ , the scale height  $z_0 = 0.5 \text{ kpc}$  for these clusters at  $r = 2\alpha^{-1} =$

$3.3$  or  $3.2 \text{ kpc}$ , where  $\alpha^{-1}$  is the disk scale length for the LMC exponential disk. Hence our data suggest that, quite unlike our own Galaxy, *there is no evidence for a kinematic halo population among the globular clusters in the LMC.*

We are very grateful to A. Cowley, D. Hartwick, L. Searle, and H. Smith for the use of their unpublished data and to P. Schechter for the use of a nonlinear regression routine. We thank D. S. Mathewson for very helpful comments, G. de Vaucouleurs for useful discussions, and B. J. Bok for his encouragement. A. O. and G. D. I. gratefully acknowledge the hospitality of the Mount Stromlo and Siding Springs Observatory during part of the course of this work. One of us (G. D. I.) regrets that no way was found to incorporate a  $V/\sigma$ - $\epsilon$  figure in this paper. This work was supported in part by the Alfred P. Sloan Foundation and by the National Science Foundation under grant AST80-12915.

## REFERENCES

- Aaronson, M., and Mould, J. 1982, *Ap. J. Suppl.*, **48**, 161.  
 Abt, H. A., and Biggs, E. S. 1972, *Bibliography of Stellar Radial Velocities* (Tucson: Kitt Peak National Observatory).  
 Andrews, P. J., and Lloyd Evans, T. 1972, *M.N.R.A.S.*, **159**, 445 (AE).  
 Bernard, A. 1975, *Astr. Ap.*, **40**, 199.  
 Bernard, A., and Bigay, J. H. 1974, *Astr. Ap.*, **33**, 123.  
 Bevington, P. R. 1969, *Data Reduction and Error Analysis for the Physical Sciences* (New York: McGraw Hill).  
 Cheriguene, M. F. and Monnet, G. 1972, *Astr. Ap.*, **16**, 28.  
 Cowley, A. P., and Hartwick, F. D. A. 1981a, private communication.  
 ———. 1981b, *A.J.*, **86**, 667.  
 ———. 1982, *Ap. J.*, **259**, 89 (CH).  
 de Vaucouleurs, G. 1957, *A.J.*, **62**, 69.  
 de Vaucouleurs, G., and Freeman, K. C. 1973, *Vistas in Astronomy*, ed. A. Beer, Vol. **14**, p. 163.  
 Feast, M. W. 1968, *M.N.R.A.S.*, **140**, 345.  
 Feitzinger, J. V., Isserstedt, J., and Schmidt-Kahler, Th. 1977, *Astr. Ap.*, **57**, 265.  
 Feitzinger, J. V., and Weiss, G. 1979, *Astr. Ap. Suppl.*, **37**, 575.  
 Ford, H. C. 1970, Ph.D. thesis, University of Wisconsin.  
 Freeman, K. C. 1970, *Ap. J.*, **160**, 811.  
 ———. 1980, in *IAU Symposium 85, Star Clusters*, ed. J. D. Hesser (Dordrecht: Reidel), p. 317.  
 Freeman, K. C., and Carrick, D. 1969, unpublished study.  
 Frenk, C. S., and Fall, S. M. 1982, *M.N.R.A.S.*, **199**, 565.  
 Frenk, C. S. and White, S. D. M., 1980, *M.N.R.A.S.*, **193**, 295.  
 Gascoigne, S. B. C. 1980, in *IAU Symposium 85, Star Clusters*, ed. J. D. Hesser (Dordrecht: Reidel), p. 305.  
 Geisler, D., and Hodge, P. 1980, *Ap. J.*, **242**, 66.  
 Graham, J. A. 1973, in *IAU Colloquium 21, Variable Stars in Globular Clusters and Related Systems*, ed. J. D. Fernie (Dordrecht: Reidel), p. 120.  
 Hodge, P. 1960, *Ap. J.*, **131**, 351.  
 ———. 1981, in *IAU Colloquium 68, Astrophysical Parameters for Globular Clusters*, ed. A. G. D. Philip and D. S. Hayes (Schenectady: Davis), p. 205.
- Hunter, C., and Toomre, A. 1969, *Ap. J.*, **155**, 747.  
 Kinman, T. D. 1959, *M.N.R.A.S.*, **119**, 157.  
 Lin, D. N. C., and Lynden-Bell, D. 1982, *M.N.R.A.S.*, **198**, 707.  
 Mathewson, D. S., Ford, V. L., Schwarz, M. P., and Murray, J. D. 1979, in *IAU Symposium 84, Large Scale Characteristics of the Galaxy*, ed. W. B. Burton (Dordrecht: Reidel), p. 547.  
 Mathewson, D. S., and Schwarz, M. P. 1976, *M.N.R.A.S.*, **176**, 47P.  
 Mathewson, D. S., Schwarz, M. P., and Murray, J. D. 1977, *Ap. J. (Letters)*, **217**, L5.  
 McGee, R. X., and Milton, J. A. 1966, *Australian J. Phys., Ap. Suppl.*, **2**.  
 Prevot, L. 1973, *Astr. Ap.*, **28**, 165.  
 Searle, L. 1981, private communication.  
 Searle, L., and Smith, H. 1983, in preparation (SS).  
 Searle, L., Wilkinson, A., and Bagnuolo, W. G. 1980, *Ap. J.*, **239**, 803 (SWB).  
 Shapley, H., and Lindsay, E. M. 1963, *Irish Astr. J.*, **6**, 74.  
 Smith, M. G., and Weedman, D. W. 1971, *Ap. J.*, **169**, 271.  
 ———. 1972, *Ap. J.*, **177**, 595.  
 Stryker, L. L. 1981, Ph.D. thesis, Yale University.  
 Sulentic, J. W., and Tifft, W. G. 1973, *The Revised New General Catalogue of Nonstellar Astronomical Objects* (Tucson: The University of Arizona Press).  
 Thackeray, A. D. 1974, *M.N.A.S. South Africa*, **33**, 66.  
 Tubbs, A. D., and Sanders, R. H. 1979, *Ap. J.*, **230**, 736.  
 van den Bergh, S. 1981, *Astr. Ap. Suppl.*, **46**, 79.  
 van der Kruit, P. C., and Searle, L. 1981, *Astr. Ap.*, **95**, 105.  
 Webbink, R. F. 1981, *Ap. J. Suppl.*, **45**, 259.  
 Wood, P. R. 1981, private communication.  
 Wood, P. R., and Cahn, J. H. 1977, *Ap. J.*, **211**, 499.  
 Zinn, R. 1980a, *Ap. J. Suppl.*, **42**, 19.  
 ———. 1980b, *Ap. J.*, **241**, 602.

K. C. FREEMAN: Mount Stromlo and Siding Spring Observatory, Private Bag, Woden P.O., A.C.T. 2606, Australia

GARTH D. ILLINGWORTH: Kitt Peak National Observatory, P.O. Box 26732, Tucson, AZ 85726

A. OEMLER, JR.: Department of Astronomy, Yale University, P.O. Box 6666, New Haven, CT 06511